Biomedicine & Pharmacotherapy 102 (2018) 653–669

Contents lists available at ScienceDirect

Biomedicine & Pharmacotherapy

journal homepage: www.elsevier.com/locate/biopha

Oncogenic long noncoding RNA MALAT1 and HCV-related hepatocellular carcinoma

Eman A. Toraih[a,b,*], Alia Ellawindy[a], Salma Y. Fala[c], Essam Al Ageeli[d], Nawal S. Gouda[e], Manal S. Fawzy[f,g,**], Somaya Hosny[b,h]

[a] Genetics Unit, Department of Histology and Cell Biology, Faculty of Medicine, Suez Canal University, Ismailia, Egypt
[b] Center of Excellence of Molecular and Cellular Medicine, Suez Canal University, Ismailia, Egypt
[c] Faculty of Medicine, Suez Canal University, Ismailia, Egypt
[d] Department of Clinical Biochemistry (Medical Genetics), Faculty of Medicine, Jazan University, Jazan, P.O. 45142, Saudi Arabia
[e] Department of Medical Microbiology and Immunology, Faculty of Medicine, Mansoura, Mansoura University, Egypt
[f] Department of Medical Biochemistry, Faculty of Medicine, Suez Canal University, Ismailia, P.O. 41522, Egypt
[g] Department of Biochemistry, Faculty of Medicine, Northern Border University, Arar, Saudi Arabia
[h] Department of Histology and Cell Biology, Faculty of Medicine, Suez Canal University, Ismailia, Egypt

ARTICLE INFO

Keywords:
MALAT1
HCV
HCC
lncRNA
Meta-analysis

ABSTRACT

Hepatocellular carcinoma (HCC) is the second leading cause of cancer-related mortality worldwide. The oncogenic function of the long non-coding RNA; metastasis-associated lung adenocarcinoma transcript 1 (MALAT1) in HCC remains unclear. We aimed to evaluate MALAT1 serum expression profile in HCC and explore its relation to the clinicopathological features. Quantitative Real Time-Polymerase Chain Reaction was applied in 70 cohorts (30 HCC, 20 HCV, 20 controls). Further meta-analysis of clinical studies and *in vitro* validated experiments was employed. Serum MALAT1 showed area under the curve of 0.79 and 0.70 to distinguish patients with cancer from normal and cirrhotic individuals at fold change of 1.0 and 1.26, respectively. Expression level was significantly higher in males ($P < 0.001$) and patients with massive ascites ($P = 0.005$). Correlation analysis showed positive correlation of MALAT1 with total bilirubin (r = 0.456, $P < 0.001$) and AST (r = 0.280, $P = 0.019$), and negative correlation with the hemoglobin level (r = 0.312, $P = 0.009$). Meta-analysis showed that the over-expressed MALAT1 was linked to tumor number [Cohen's d = 0.450, 95% CI (0.21 to 0.68)], clinical stage [Cohen's d = 0.048, 95% CI (-0.83 to 0.74)], and AFP level [Cohen's d = 0.354, 95% CI (0.1 to 0.57)]. *In silico* data analysis and systematic review confirmed MALAT1 oncogenic function in cancer development and progression.

In conclusion, circulatory MALAT1 might represent a putative non-invasive prognostic biomarker indicating worse liver failure score in HCV-related HCC patients with traditional markers. Large-scale verification is warranted in future studies.

1. Introduction

Hepatocellular Carcinoma (HCC) is considered the sixth most commonly diagnosed type of cancer worldwide [1] and the second leading cause of cancer-related mortality [2]. Hepatitis C virus (HCV) is proposed to be one of the major risk factors for HCC worldwide [3], about 1–4% per year of HCV-infected cirrhotic patients are expected to develop malignant transformation in hepatocytes [3,4]. In Egypt, the prevalence of chronic liver disease due to HCV infection represents 13.8% of the whole population, and up to 80% of liver cancer patients

Abbreviations: AFP, alpha fetoprotein; AUC, area under the ROC curve; cDNA, complementary DNA; DRAIC, Down-regulated RNA In Cancer; EMT, epithelial-mesenchymal transition; eRNAs, enhancer RNAs; EZH2, Enhancer Of Zeste 2 Polycomb Repressive Complex 2 Subunit; GAS5, growth arrest specific 5; HCC, Hepatocellular carcinoma; HCN, Hepcarcin; HCV, Hepatitis C virus; HEIH, Highly Expressed In Hepatocellular Carcinoma Long Non-Coding RNA; HULC, hepatocellular carcinoma up-regulated long non-coding RNA; ITGB1, Integrin β1; LINC00047, Long Intergenic Non-Protein Coding RNA 47; lncRNAs, long non-coding RNAs; LTBP3, latent transforming growth factor β-binding protein 3; MALAT1, metastasis-associated lung adenocarcinoma transcript 1; mascRNA, MALAT1-associated small cytoplasmic RNA; ncRNA-a, activating ncRNAs; NEAT2, Nuclear Enriched Abundant Transcript 2; OncoLncs, oncogene long non-coding RNAs; plncRNAs, promotor-associated long RNAs; PRC, polycomb repressive complex; ROC, Receiver operating characteristic; RT-PCR, Reverse transcription-Polymerase Chain Reaction; siRNA, small interfering RNA; TF, transcription factors; TS, thymidylate synthase; TSLncs, tumor suppressor long non-coding RNAs

* Corresponding author at: Genetics Unit, Department of Histology and Cell Biology, Faculty of Medicine, Suez Canal University, Ismailia, Egypt.
** Corresponding author at: Department of Biochemistry, Faculty of Medicine, Northern Border University, Arar, Saudi Arabia.
E-mail addresses: emantoraih@med.suez.edu.eg (E.A. Toraih), manal_mohamed@med.suez.edu.eg (M.S. Fawzy).

https://doi.org/10.1016/j.biopha.2018.03.105
Received 21 November 2017; Received in revised form 11 March 2018; Accepted 17 March 2018
0753-3322/ © 2018 Elsevier Masson SAS. All rights reserved.

have underling hepatitis C [5].

HCV has seven major genotypes that vary according to the geographic area. Genotype-4, in particular, is confined to the Middle East region, accounting for up to 90% of HCV Egyptian patients and about 15% of total global HCV infection [5]. Despite numerous studies on HCC, there are no effective biomarkers for the early tumor detection and prognosis and most cases are diagnosed at an advanced or a non-resectable stage at presentation leading to lower survival rate [6]. Thus, it is extremely necessary to discover new biomarkers for precise diagnosis, prognosis, and treatment of HCV-related HCC.

Recently, long non-coding RNAs (lncRNAs) have been implicated in the pathogenesis of liver diseases [7]. They are non-coding transcripts longer than 200 nucleotides [8], that are transcribed by RNA polymerase II, followed by 5′ capping, 3′ polyadenylation, and splicing similar to protein-coding genes [9]. LncRNAs can be classified according to their genomic location. For instance, they can be found overlapping protein-coding genes or exist in distinct intergenic regions with separate transcriptional units from annotated coding region. Other types include promoter-associated long RNAs (plncRNAs), telomeric-repeat containing RNA and transcribed ultra-conserved RNAs [10,11]. They can be transcribed from sense, antisense or both strands relative to the promoter of a protein-coding gene. Additionally, lncRNAs can be categorized according to their function into enhancer RNAs (eRNAs), which interact with enhancer regions, and activating ncRNAs (ncRNA-a) which have an enhancer like effects. Finally, they can also be classified according to their structure into linear or circular, with the latter being generated by back-splicing of introns of mRNAs [11].

To date, in human, 146,742 lncRNAs were identified and annotated in LNCipedia database version 4.1 (https://lncipedia.org/). Accumulating evidence indicates that lncRNAs can play crucial roles in various pathological states. They can regulate cancer-related genes at transcriptional, post-transcriptional and epigenetic levels; through modulating mRNA splicing, stability, degradation, and translation [8] and regulating epigenetic mechanisms and nuclear organization [11]. They can act as scaffolds for chromatin-protein complexes, recruit histone-modifying enzymes to chromatin, regulate DNA methylation, and induce chromatin modifications [12]. lncRNAs have been found to be deregulated in liver cancer [8]. Interestingly, they can behave like oncogenes (OncoLncs) or tumor suppressors (TSLncs) [9,13]. For example, over-expression of HULC (hepatocellular carcinoma up-regulated long non-coding RNA) and HEIH (Highly Expressed in Hepatocellular Carcinoma Long Non-Coding RNA) was correlated with HCC development or progression, whereas, DRAIC (Down-regulated RNA In Cancer) and GAS5 (growth arrest specific 5) down-regulation may act as a tumor suppressor in a variety of human cancers [14].

In the past decades, emerging evidence suggested the association of the lncRNA Metastasis-Associated Lung Adenocarcinoma Transcript 1 (MALAT1) with a wide variety of cancers; including lung cancer [15], osteosarcoma [16], glioblastoma multiforme [17], and hepatocellular carcinoma [18]. Human *MALAT1* gene (ENSG00000251562) is located along the long arm of chromosome 11q13.1 on the forward strand spanning 8.75 Kb long (11: 65,497,762-65,506,516; according to GRCh38). It has other synonyms; including Hepcarcin (HCN), Nuclear Enriched Abundant Transcript 2 (NEAT2), and Long Intergenic Non-Protein Coding RNA 47 (LINC00047). The precursor RNA of MALAT1 is first transcribed by RNA polymerase II (RNA Pol II) then cleaved by RNase P enzyme from its 3-prime end into two parts to yield a large nuclear-retained lncRNA and MALAT1-associated small cytoplasmic RNA (mascRNA) localized exclusively in the cytoplasm. The long ncRNA partly lacks poly(A) tail, but is stabilized by its U-rich motifs [19]. Due to alternative splicing, *MALAT1* gene can encode 17 different lncRNA transcripts ranging from 132 to 8708 bp in length (www.Ensembl.org) (Fig. 1). They are mainly accumulating in distinct zones called nuclear speckles that regulate post-transcriptional RNA processing machinery; namely pre-mRNA splicing and mRNA export. The long transcripts are highly abundant; about 3000 copies/cell [20]. They act as molecular scaffolds for ribonucleoprotein complexes, transcriptional regulators for numerous genes, including those involved in cancer metastasis and cell migration, and key modulators in cell cycle regulation. On the other hand, the small ncRNA originates from a highly conserved region. After processing, it folds into a tRNA-like cloverleaf, followed by the addition of a CCA motif by the RNase Z enzyme. Unlike the nuclear transcript, the mascRNA has a relatively short half-life. It is thought to act as a "sponge" for proteins, preventing them from reaching their natural destinations within the cell [21].

To assess the diagnostic and prognostic value of MALAT1 as a non-invasive biomarker in combination with alpha fetoprotein (AFP) in hepatocellular carcinoma, we examined the expression profile of the lncRNA MALAT1 in the circulation of liver cancer patients compared to normal and cirrhotic cohorts. Additionally, a comprehensive *in silico* analysis was employed to explore the biological features and the clinical implications of the OncoLnc MALAT1 in hepatic carcinogenesis aiming at providing insights into precision in diagnosis and treatment of HCC.

2. Materials and methods

2.1. In silico structural and functional analysis of MALAT1

Structural genomics analyses of *MALAT1* gene and transcripts were retrieved from online databases as Ensemble.org and GeneCards.com. COMPARTMENTS subcellular localization database was investigated to identify the subcellular localization of MALAT1 RNA (compartments.jensenlab.org/). Functional gene ontology was assessed by lncRNA2function (https://mlg.hit.edu.cn/lncrna2function/). Transcription factors binding sites were determined (Genecard.org). Protein-protein interaction was identified using STRING database version 10.0 (Search Tool for the Retrieval of Interacting Genes/Proteins). Starbase (http://starbase.sysu.edu.cn/), microRNA.org, and Diana-LncBase v2.0 (http://carolina.imis.athena-innovation.gr/) were used to identify protein and RNA inter-actors with MALAT1.

2.2. Expression profile analysis

2.2.1. Study participants

A total of 70 individuals were enrolled in the study (20 controls, 20 patients with liver cirrhosis (LC) caused by HCV infection, and 30 patients with hepatocellular carcinoma on top of HCV). The control group was obtained from healthy blood bank donors. They matched the other two groups in age, gender, and residence, and had no history of any concomitant infection or chronic illness. Patients were recruited from the General Surgery and Oncology Department, Suez Canal University Hospital, Egypt, during the period between January 2017 and July 2017.

2.2.2. Ethical approval

The study was conducted according to the ethical guidelines of the 1964 Declaration of Helsinki (2008 revision), and approved by the Medical Research Ethics Committee of Suez Canal University (Research ID 3137). Informed consent was obtained from participants prior to blood sampling.

2.2.3. Patient assessment

All the patients included in the study had clinical and radiological evidence suggestive of cirrhosis and confirmation of HCV infection by detection of HCV RNA in their serum. Patients with non-HCV induced HCC, other autoimmune or metabolic liver diseases were excluded. Liver cancer had typical imaging findings and elevated serum alpha fetoprotein (AFP). Patients with HCC underwent thorough clinical examination, abdominal ultrasonography, quantitative assessment of viral load by PCR, Barcelona-Clinic Liver Cancer (BCLC) staging, and prognostic assessment by Child-Turcotte-Pugh (CTP) scoring tool [22].

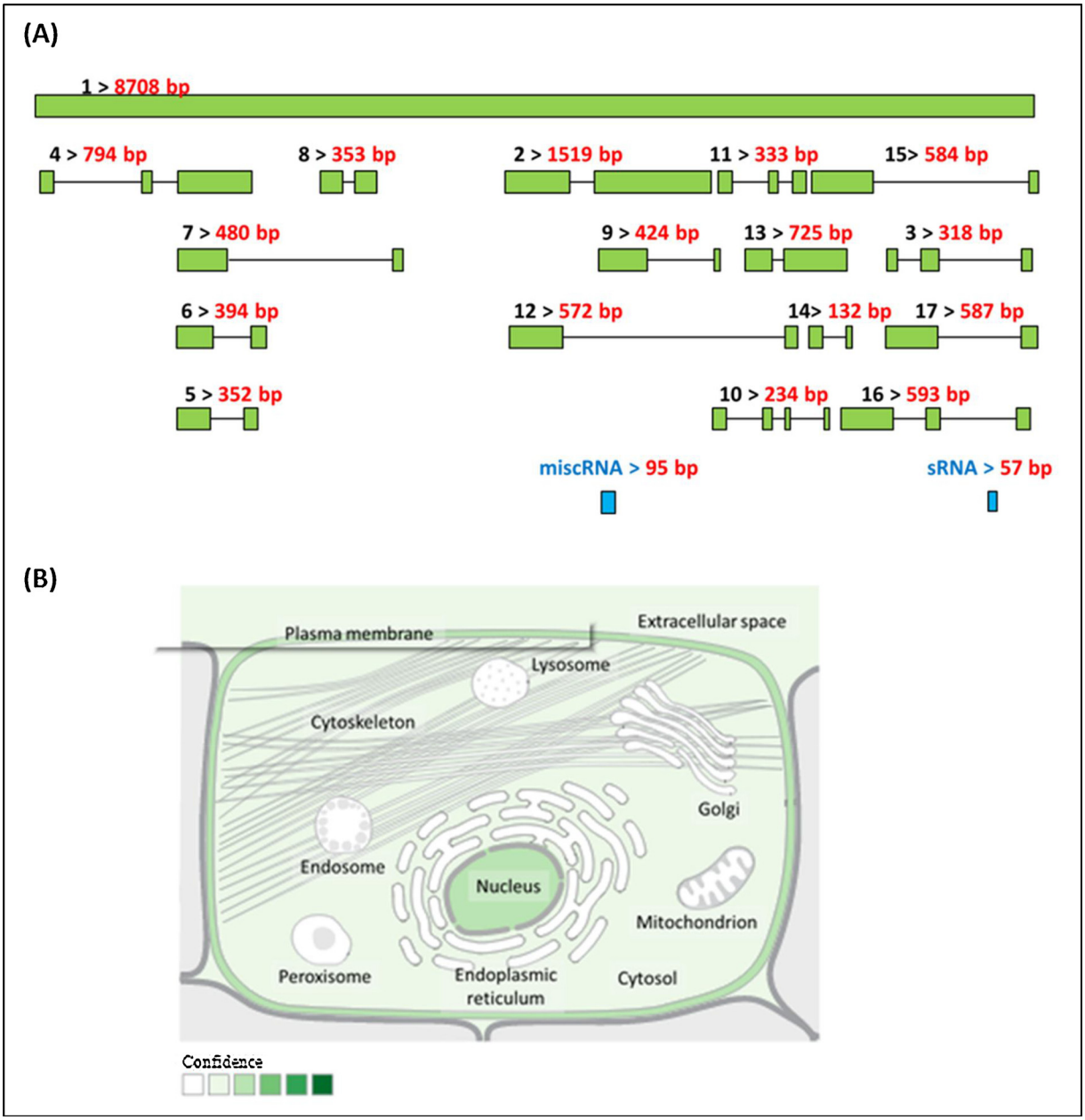


Fig. 1. *MALAT1* gene transcripts. (A) Alternative splicing of *MALAT1* gene. The transcript is represented in green box, the number of the transcript in black, and the length of the transcripts in base pair (bp) in red [Data source: ensemble.com]. (B) Subcellular localization of MALAT1 transcripts. The darker the green colour the higher the confidence of the localization of MALAT1 in the cell based on database annotations, automatic text mining of the biomedical literature, and sequence-based predictions [Data source: http://compartments.jensenlab.org/].

2.2.4. Specimen collection

Fasting blood samples were withdrawn from the study participants and subdivided in plain tubes, sodium citrate (200 µl of 3.8%) anticoagulant tubes, and trisodium EDTA (1 mg/ml) tubes. The plain and citrated tubes were centrifuged at 1500 x g for 10 minutes. Part of the citrated plasma was used in prothrombin time (PT) analysis immediately and the rest of plasma and the serum were apportioned into 0.5 ml aliquots and stored at −20 °C.

2.2.5. Laboratory investigations

An enzymatic method on the automated Hitachi-912 analyzer (Roche Diagnostics Co, Mannheim, Germany) was run for fasting blood glucose (FBG), serum alanine transaminase (ALT), serum aspartate transaminase (AST), alkaline phosphatase (ALP), serum total bilirubin and albumin analyses. Serum AFP concentration was measured by the chemiluminescent immunometric assay on Siemens IMMULITE® 2000 (Siemens Healthcare Diagnostics, USA). An automated cell counter (Cell Dyne-2700, Abbott Lab, USA) was used for hemoglobin (Hb) estimation, white blood cells (WBC) count and platelet count detection. Prothrombin concentration was measured using an automated analyzer (Sysmex CA-1500, USA).

2.2.6. RNA extraction

Extraction of total RNA from whole blood was carried out using PureLink® RNA Mini Kit (Qiagen, Catalog no. 217,184) according to the manufacturer's instruction. RNA concentration and purity were assessed *via* NanoDrop ND-1000 spectrophotometer (NanoDrop Tech., Inc. Wilmington, DE, USA).

Table 1
Demographic, clinical, and biochemical characteristics of the study groups.

Variables	Normal	LC	HCC	*P* values
Number	20	20	30	
Age				
Age, mean (SD)	52.1 ± 13.7	51.8 ± 14.7	53.4 ± 12.4	0.907
Age groups (y)				
< 55 y	10 (50.0)	11 (55.0)	13 (43.3)	0.713
≥55 y	10 (50.0)	9 (45.0)	17 (56.7)	
Gender				
Females	9 (45.0)	8 (40.0)	11 (367)	0.841
Males	11 (55.0)	12 (60.0)	19 (63.3)	
Family history of cancer	1 (5.0)	4 (20.0)	4 (13.3)	0.364
Obesity	5 (25.0)	7 (35.0)	8 (26.7)	0.747
Diabetes mellitus	4 (20.0)	6 (300)	6 (20.0)	0.667
Hypertension	2 (10.0)	3 (15.0)	5 (16.7)	0.800
CLD features				
Jaundice	——	20 (100)	30 (100)	NA
Pallor	——	18 (90.0)	30 (100)	0.077
Purpura	——	18 (90.0)	20 (66.7)	0.058
Spider nevi	——	16 (80.0)	30 (100)	**0.011**
Gynamcomastia	——	1 (5.0)	21 (70.0)	< **0.001**
Palmer erythema	——	16 (80.0)	30 (100)	**0.011**
Flapping tremors	——	10 (50.0)	22 (73.3)	0.092
Lower limb edema	——	16 (80.0)	16 (53.3)	0.054
Hepatomegaly	——	16 (80.0)	12 (40.0)	**0.005**
Splenomegaly	——	20 (100)	30 (100)	NA
Hernia	——	15 (75.0)	21 (70.0)	0.700
Encephalopathy	——	1 (25.0)	26 (86.6)	< **0.001**
LCF score	——	5.85 ± 0.8	9.7 ± 1.2	< **0.001**
CTP class				
Child A	——	16 (80.0)	0 (0.0)	< **0.001**
Child B	——	4 (20.0)	21 (70.0)	
Child C	——	0 (0.0)	9 (30.0)	
Radiological findings				
Hepatomegaly				
Mild	——	4 (20.0)	18 (60.0)	**0.005**
Massive	——	16 (800)	12 (40.0)	
Liver surface				
Smooth	——	19 (95.0)	30 (100)	0.216
Irregular	——	1 (5.0)	0 (0.0)	
Splenomegaly	——	2 (10.0)	3 (10.0)	1.00
Portal hypertension				
Portal vein	——	20 (100)	30 (100)	NA
Hepatic vein	——	3 (15.0)	7 (23.3)	0.470
Splenic vein	——	18 (900)	30 (100)	0.077
Gall bladder stone	——	5 (25.0)	14 (46.7)	0.122
Ascites	——	7 (35.0)	30 (100)	< **0.001**
Tumor characteristics				
Maximum tumor size, cm	——	——	7.26 ± 3.7	
< 5 cm	——	——	9 (30.0)	
≥5 cm	——	——	21 (70.0)	
Number of lesions	——	——		
Solitary	——	——	20 (66.7)	
Multiple	——	——	10 (33.3)	
Laboratory data				
AST (U/L)	41.5 ± 2.5	132.4 ± 33.7 #	168.1 ± 64.4 #*	< **0.001**
ALT (U/L)	27.8 ± 49	140.3 ± 29.8 #	145.2 ± 306 #	< **0.001**
Bilirubin (mg/dl)	0.62 ± 0.9	1.70 ± 0.5	3.44 ± 0.7	< **0.001**
Albumin (g/l)	4.45 ± 0.9	3.89 ± 0.4 #	3.46 ± 0.5 #*	< **0.001**
FBS (mmol/l)	8.04 ± 1.6	7.08 ± 1.6 #	8.19 ± 1.6 #	0.063
AFP (μg/l)	6(2.7-11.5)	140(112-150.7)	789(658-1226) #	< **0.001**
HB (g/dl)	10.5 ± 1.7	9.91 ± 1.5	9.27 ± 1.54 #	**0.036**
WBC (x10^9/l)	4.44 ± 1.44	5.25 ± 2.5	5.11 ± 2.1	0.418
PLT (x10^9 /l)	138.3 ± 30.1	131.9 ± 45.9	109.9 ± 32.0	**0.017**
PT (sec)	14.6 ± 7.3	12.8 ± 2.1	14.9 ± 2.4	0.241
Abnormal INR	0 (0.0)	0 (0.0)	8 (26.7)	**0.012**

Data are shown as number (percentage) or mean ± standard deviation. LC: liver cirrhosis; HCC, hepatocellular carcinoma patients; CTP, Child-Turcotte-Pugh classification for liver cell failure; LCF, liver cell failure score by CTP classification; ALT, alanine transaminase; AST, aspartate transaminase; PT, prothrombin time; AFP, alpha fetoprotein; HB, hemoglobin count; WBC, while blood cells; PLT, platelet count; INR, international normalized ratio. Chi-square, Kruskal Wallis, and ANOVA tests were used followed by Tukey multiple comparison test. # compared to normal, * compared to LC. Bold values indicate significance at $P < 0.05$.

2.2.7. Reverse transcription reaction

RNA was converted to complementary DNA (cDNA) using high capacity cDNA Reverse Transcription Kit (Applied Biosystems, P/N 4,368,814) as described in our previous work [23]. Reverse transcription (RT) reactions were carried out in a Mastercycler Gradient Thermocycler (Eppendorf, Hamburg, Germany) at 25 °C for 10 min, 37 °C for 120 min, and 85 °C for 5 min, then hold at 4 °C. Appropriate positive and negative controls were included.

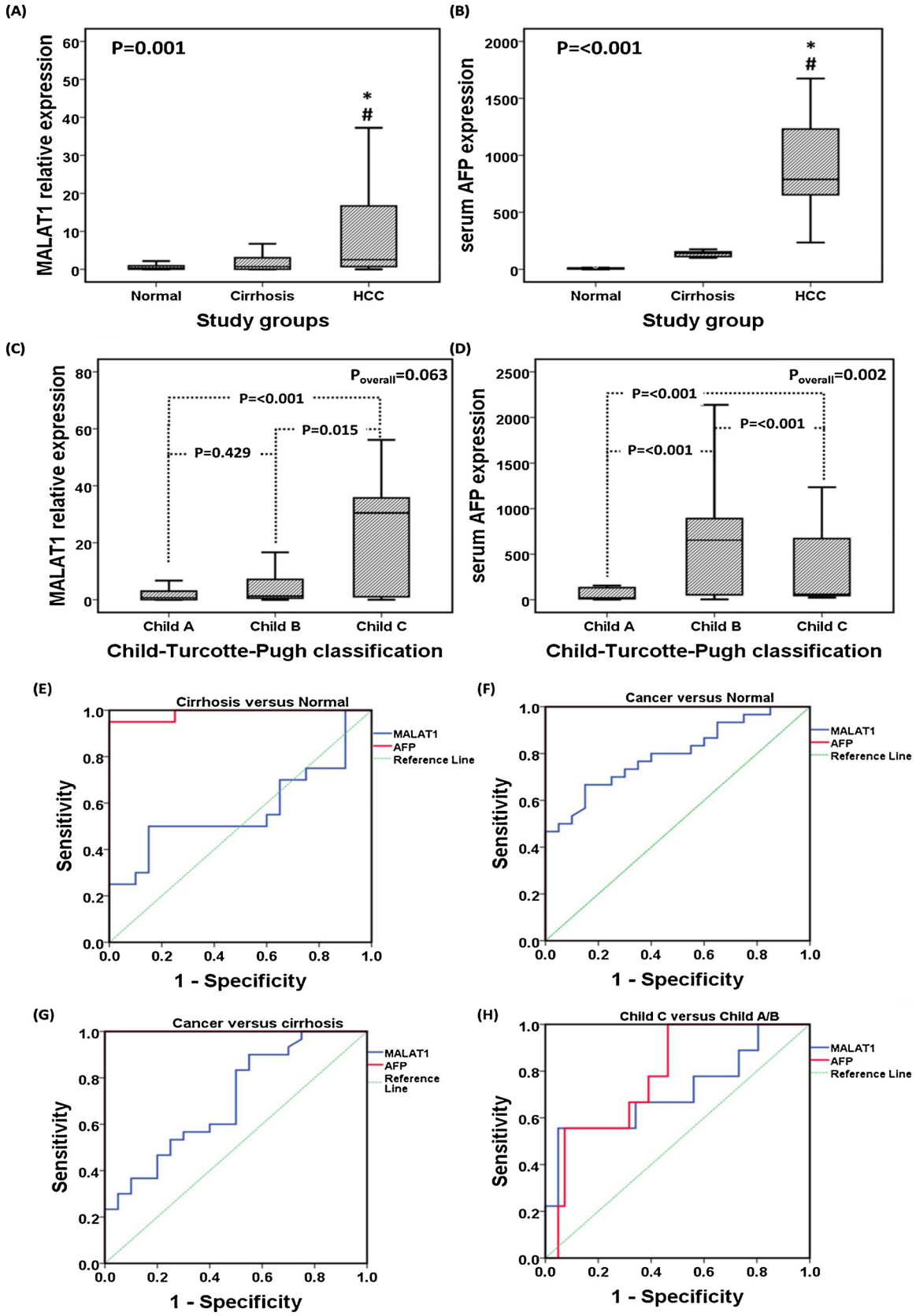


Fig. 2. Serum MALAT1 and AFP levels in liver cirrhosis and cancer.(A–D) Expression profile of circulatory MALAT1 and AFP in normal, cirrhosis and cancer individuals according to the disease severity. Data are represented as medians. The box defines upper and lower quartiles (25% and 75%, respectively) and the error bars indicate upper and lower adjacent limits. The relative expression of MALAT1 was normalized to GAPDH and calculated using the delta-delta CT method [= $2^{(-\Delta\Delta CT)}$] in comparison to normal controls. Kruskal-Wallis test followed by Mann-Whitney U test were applied for multiple comparison. # compared to normal, * compared to LC. (E–H) ROC analysis to discriminate between the study groups and to differentiate between class C disease and milder degrees.

Table 2
The diagnostic and prognostic performance of the best cutoff values of serum AFP and MALAT1 for discriminating the study groups.

	Cutoff value	AUC (95% CI)	Sensitivity (%)	Specificity (%)	P values
Cirrhosis *versus* Normal					
MALAT1	1.00	0.57 (0.38-0.76)	50.0	80.0	0.417
AFP	65.0	0.98 (0.96-1.00)	95.0	100	< **0.001**
HCC *versus* Normal					
MALAT1	1.00	0.79 (0.67-0.91)	66.7	80.0	< **0.001**
AFP	131	1.00 (1.0-1.0)	100	100	< **0.001**
HCC *versus* cirrhosis					
MALAT1	1.26	0.70 (0.55-0.85)	60.0	60.0	**0.015**
AFP	205	1.00 (1.0-1.0)	100	100	< **0.001**
Child C *versus* Child B					
MALAT1	2.54	0.71 (0.49-0.92)	66.7	65.9	**0.047**
AFP	672	0.78 (0.63-0.92)	77.8	61.0	**0.008**

AFP: alpha-fetoprotein; AUC; area under the curve; CI: confidence interval. Bold values indicate significance at $P < 0.05$.

2.2.8. Gene expression analysis

Gene expression of *MALAT1* compared to *GAPDH* was performed using Real-Time Reverse transcription-Polymerase Chain Reaction (RT-PCR) technology in accordance with the Minimum Information for Publication of Quantitative Real-Time PCR Experiments (MIQE) guidelines [24]. The PCR reactions were carried out in triplicate with a final volume of 20 µl, including 1.33 µl RT product, 2× TaqMan® Universal PCR Master Mix (Applied Biosystems, P/N 4,440,043), 1 µl TaqMan® assays (Hs00273907_s1 or Hs02786624_g1) using the conditions described in a prior publication [25].

2.2.9. Statistical analysis

Data were handled using R packages and SPSS v. 22. Multivariate analysis of the whole study population and independent variables (age, gender, biochemical investigations, AFP, and MALAT1) was carried out for data exploration and clustering using PC-ORD version 6.0 [26]. Chi-square (χ^2) or Fisher's exact tests were used for categorical data, while Mann-Whitney U (MW) and Kruskal-Wallis (KW) tests were conducted to assess the difference between continuous variables. Pearson's correlation analysis was conducted to determine the correlation between the lncRNA MALAT1 and the clinical and biochemical parameters. A two-tailed *P*-value was considered statistically significant at a value of < 0.05. Receiver operating characteristic (ROC) and the area under the ROC curve (AUC) were applied to identify the diagnostic and prognostic performance value of *MALAT1* and *AFP* expression levels. The fold change of the current lncRNA expression was estimated using the following equation: relative quantity $= 2^{-\Delta\Delta CT}$.

2.3. Meta-analysis

We were interested to compare our findings with the previous ones by a systematic way. Hence, we followed the PRISMA statement [27] and MOOSE-guidelines [28] to prepare a systematic review and meta-analysis of the previous observational analysis.

2.3.1. Search strategy

We searched Web of Science, Science direct, Scopus, National institutes of health (NIH) and the Cochrane Library with no restriction on the date of the publication through July 2017 using the following search terms: (“Metastasis-Associated Lung Adenocarcinoma Transcript 1″ OR "MALAT1″ OR "Long noncoding RNA MALAT1″ OR "MALAT-1″ OR "MALAT 1″) AND ("Hepatic" OR "liver" OR “hepatocellular) AND ("cancer" OR "tumor" OR "carcinoma"). Moreover, we searched PubMed using the following search term: (“"MALAT1″ OR "MALAT-1″ OR "MALAT 1″) AND ("Hepatic" OR "liver" OR “hepatocellular”) AND ("cancer" OR "tumor" OR "carcinoma").

2.3.2. Inclusion and exclusion criteria

Studies satisfying the following criteria were included in our review: (1) studies where the association between MALAT1 expression and HCC was investigated; (2) those where the expression levels of MALAT1 were measured in HCC samples compared to control samples; and (3) ones with an adequate description of the clinico-pathological features of the included population. Exclusion criteria were the following: (1) letters, editorials, expert opinions and case reports; (2) non-original articles; (3) studies with overlapped or unreliable data; and (4) duplication.

2.3.3. Data extraction

Study reviewers extracted data from eligible studies to a uniform data extraction sheet. Extracted data included the following items: the first author, year of publication, country, number of patients, the number and pathological features of the high and low MALAT1 expression groups, and the detection method of the lncRNA MALAT1, age of HCC patients, gender, tumor number, tumor size, the clinical stage of the tumor, AFP level, and tumor differentiation. The Cohen’s d values of the relation between MALAT1 expression level and the clinico-pathological features were estimated by three methods. In the first method, *P* value was obtained from studies that used Chi-square or Fisher's Exact tests, and then calculated Cohen’s d and its variance were employed using the online Campbell tool (https://www.campbellcollaboration.org/). The second method involved applying the Chi-square test on the reported number of events, then calculating its Cohen’s d and variance. In the third method, we applied the Chi-square test using the mean and standard deviation mentioned in the paper.

2.3.4. Quality assessment

As all the included studies were observational retrospective studies, we, therefore, assessed the quality of eligible studies using the Newcastle Ottawa Scale (NOS scale), a reliable star-based scoring system for assessing the quality of observational studies. All eligible articles were scored as reported previously [29]. Studies were scored according to (a) their design based on five items: (study objective definition, study design, outcome definition, statistical consideration, statistical method and test description); (b) laboratory methodology based on seven items (blinding in the biological assays performance, tested factor description, tissue sample conservation, description of the relevant test procedure of the biological factor, description of the negative and positive control procedures, test reproducibility control, definition of the level of positivity of the test); and (c) generalizability based on six items (patient selection criteria, patients’ characteristics, initial investigation, treatment description, source of samples, number of un-assessable samples with exclusion causes). For the scoring system, each item was scored by 2 points if it was clearly defined in the article, 1 point if its description was incomplete or unclear and 0 points if it was not defined. The maximum score for the article was 32 points.

2.3.5. Statistical analysis

The effect size (Cohen's d) was computed for all outcomes and its variance and standard error. The Cohen’s d was pooled in a fixed random effect meta-analysis model using Comprehensive meta-analysis (CMA) program V.3. Heterogeneity among the included studies was examined by Chi-square test (Q-test) and Higgins' I^2. Begg’s rank correlation and Egger’s linear regression test were employed to assess the publication bias. Two-sided *P* values at < 0.1 was considered significant.

Table 3
Clinical and pathological variables associated with the levels of MALAT1 in cirrhotic and cancer patients.

		LC	*P*	HCC	*P*
Age	< 55 y	1.23 (0.05-6.4)	0.295	3.13 (0.93-20.3)	0.805
	≥55 y	0.04 (0.01-3.02)		1.30 (0.37-23.5)	
Gender	Females	0.04 (0.01-0.15)	0.069	0.22 (0.04-0.99)	< **0.001**
	Males	1.46 (0.31-6.62)		7.16 (1.94-31.5)	
FH	Negative	0.70 (0.03-3.76)	0.820	2.32 (0.45-20.1)	0.791
	Positive	0.72 (0.01-8.78)		3.40 (1.02-28.02)	
Obesity	Negative	1.21 (0.01-6.56)	0.536	2.54 (0.74-32.6)	0.256
	Positive	0.18 (0.03-1.44)		2.85 (0.22-5.17)	
Diabetes mellitus	Negative	1.22 (0.01-6.51)	0.444	3.93 (0.87-27.0)	0.347
	Positive	0.11 (0.03-1.45)		0.85 (0.05-18.0)	
Hypertension	Negative	1.23 (0.04-5.47)	0.179	4.72 (0.90-31.0)	0.074
	Positive	0.013		0.71 (0.04-4.10)	
CTP class	Child A	0.70 (0.03-3.76)	0.554	——	0.209
	Child B	0.62 (0.01-8.73)		1.50 (0.62-8.14)	
	Child C	—		30.84 (0.55-45.9)	
CLD features					
Purpura	Negative	11.08(5.55-16.6)	0.674	1.72(0.75-13.2)	0.588
	Positive	0.70(0.03-1.53)		4.79(0.57-27.0)	
Spider nevi	Negative	0.02(0.01-556)	0.437	——	NA
	Positive	1.22(0.04-2.28)		2.54 (0.66-20.1)	
Palmer erythema	Negative	0.02(0.01-5.56)	0.437	——	NA
	Positive	1.22(0.04-2.28)		2.54(0.66-20.1)	
Flapping tremors	Negative	0.63(0.02-3.76)	0.971	0.67(0.07-13.8)	0.256
	Positive	0.71(0.03-1.48)		3.93(1.04-30.7)	
LL edema	Negative	0.70(0.03-2.28)	0.437	3.18(0.10-32.7)	0.854
	Positive	1.22(0.03-4.98)		2.54(1.01-32.7)	
Hernia	Negative	0.05(0.01-11.2)	0.933	0.81(0.09-10.9)	0.283
	Positive	1.21(0.04-1.52)		4.72(1.02-31.0)	
Encephalopathy	Negative	1.21(0.04-3.02)	0.300	1.46(0.78-28.4)	0.296
	Positive	0.013		3.13(0.37-14.1)	
Hepatomegaly	Negative	0.03(0.01-1.65)	0.335	2.54(0.94-12.8)	0.950
	Positive	1.22(0.04-2.28)		3.18(0.14-35.0)	
Liver surface	Smooth	0.18(0.02-2.99)	0.600	——	NA
	Irregular	1.54		2.54(0.66-20.1)	
Splenomegaly	Negative	0.12(0.01-1.48)	0.211	4.72(0.53-30.4)	0.315
	Positive	4.0(2.77-5.22)		0.99(0.71-30.4)	
Ascites	Mild	0.18(0.02-4.0)	0.183	1.40(0.45-7.65)	**0.005**
	Massive	1.44(0.03-149)		33.6(30.7-78.7)	
Gall bladder stone	Negative	0.05(0.01-1.44)	1.00	3.40(0.86-35.07)	0.275
	Positive	4.50(0.63-8.84)		2.21(0.10-8.27)	
Tumor characteristics					
Maximum tumor size	< 5 cm		NA	7.16(2.09-33.9)	0.086
	≥5 cm			1.30(0.17-10.3)	
Number of lesions	Solitary		NA	1.73(0.73-26.5)	0.948
	Multiple			3.93(0.41-20.1)	

LC: liver cirrhosis; HCC, hepatocellular carcinoma patients; CTP, Child-Turcotte-Pugh classification for liver cell failure; FH, Family history of cancer; LL, lower limb. Mann Whitney U test was used. Bold values indicate statistical significance at $P < 0.05$.

3. Results

3.1. In silico data findings

The human *MALAT1* gene was found to be conserved across mammalian species (ensembl.org). Unlike most types of lncRNAs, MALAT1 is ubiquitously expressed in various types of cells and tissues during development. In human cells, MALAT1 had a half-life ranging from 9 to 12 hours, relatively longer than other lncRNAs, possibly due to its triple helix 3′ end. Several interacting proteins were identified that could bind to MALAT1. Being localized in the nuclear speckles, it can bind to several pre-mRNA splicing proteins, such as SR proteins (SRF1, SRF2, SRF3, and SRF4), AGO2, DGCR8, TDP-43, U2 AF65, IBP160, and RNPS1. Online tools predicted binding sites for some of these transcription factors in the *MALAT1* promotor regions. Additionally, we identified several miRNAs binding sites within the genomic sequence of *MALAT1* (microRNA.org). Functional enrichment analysis was separately executed for each GO term and all *P* values were estimated by the hypergeometeric test and adjusted by the Benjamini-Yekutieli method. GO analysis of lncRNA MALAT1 showed its correlation to cell motility; one of its main biological processes is the positive regulation of cell movement [GO: 2000147].

3.2. The laboratory findings

3.2.1. Characteristics of the study groups

Baseline characteristics of the study participants are shown in Table 1. In the current study, a total of 70 individuals were enrolled, including 30 newly diagnosed HCC patients (19 males and 11 females) with a median age of 56 years (range 29 to 72 years old), 20 patients with HCV-induced liver cirrhosis (12 males and 8 females) with a median age of 51 years (range 23–80 years old), and 20 healthy individuals (11 males and 9 females) with a median age of 54 years (range 25 to 75 years old). Chronic liver disease manifestations as spider nevi, gynecomastia, palmer erythema, ascites and encephalopathy were more frequent in HCC group. However, a higher proportion

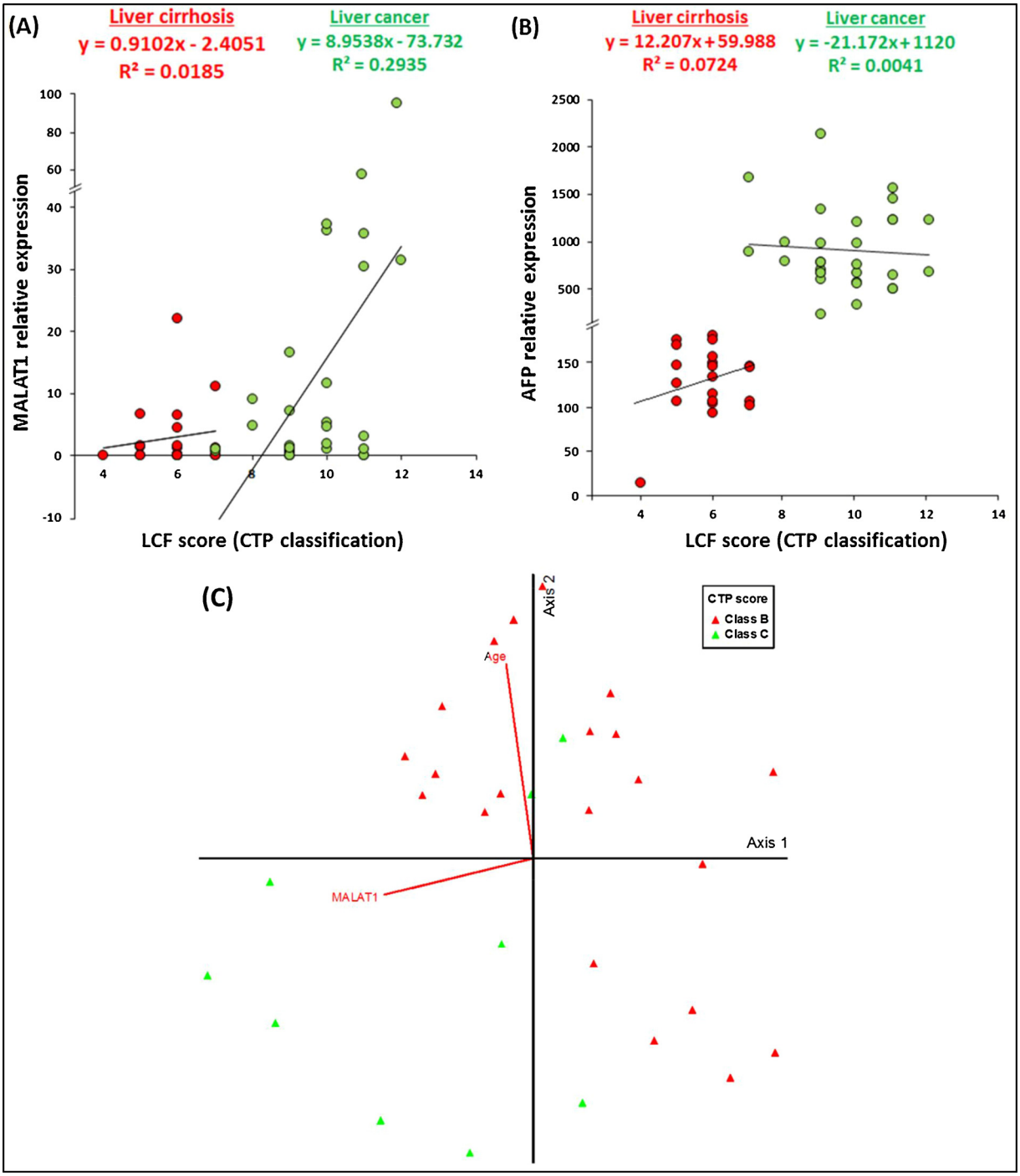


Fig. 3. Correlation analysis of serum MALAT1 and AFP with liver cell failure score in the study patients.(A) Correlation between MALAT1 and CTP score and (B) Correlation between AFP and CTP score. CTP, Child-Turcotte-Pugh classification for liver cell failure. The Pearson correlation test was used. Red and green circles represented cirrhotic and cancer patients, respectively. Regression line and equations for each patient group are shown. (C) Principal component analysis. Ordination plot of the 30 cancer patients along axis 1 and 2 revealed a tendency of higher levels of MALAT1 among CTP class C.

of LC patients had hepatomegaly. In HCV-cirrhotic group, four fifth of patients had Child A and 20% were classified as Class B. Whereas, among cancer patients, none were Child A, 70% were scored as Child B, and 30% were Child C. In HCC group, maximum tumor size of the largest diameter was 7.26 ± 3.7 cm. Two thirds of them had solitary mass by radiological assessment, while the other third had multiple masses (5 patients with 2 foci, 4 patients with 3 foci, and a single patient with 4 focal lesions). The mean values of the liver enzymes (AST and ALT), bilirubin, and AFP in the HCC group were much higher when compared to the LC group and to the healthy control group. Meanwhile, serum albumin, hemoglobin and platelet count were significantly lower in cancer and cirrhotic patients compared to controls.

3.2.2. *Transcriptomic signature in patients and controls*

The median value of MALAT1 levels in the HCC group was much higher when compared to the LC group (2.54 *versus* 0.70; $P = 0.043$) and to the healthy group (2.54 *versus* 0.32; $P = 0.025$). However, MALAT1 levels in the LC were not significantly different from normal controls ($P = 0.871$) (Fig. 2A). The prevalence of elevated serum MALAT1 (relative expression level > 1.0) was 50% in LC and 66.7% in

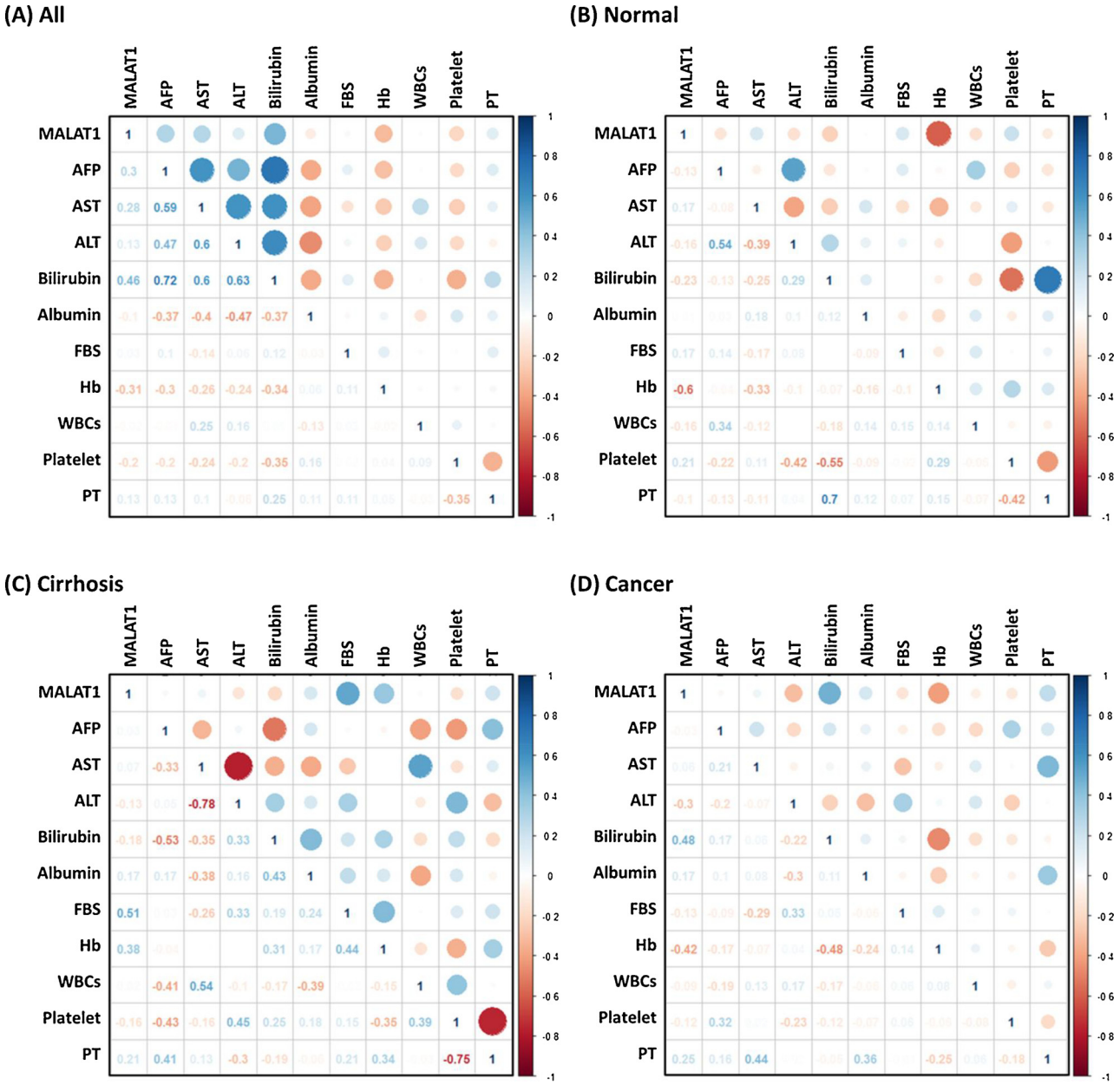


Fig. 4. Correlation analysis between biochemical features in the study groups.The Pearson correlation test was used. The correlation coefficient and direction is colored by gradient. Statistical significance at $P < 0.05$.

HCC group. Regarding the serum AFP, its median value was higher among HCC than LC group (789 *versus* 140.5; $P < 0.001$) and healthy group (789 *versus* 6.0; $P < 0.001$) (Fig. 2B). *MALAT1* profile was associated with more deterioration of liver cell function. In all patients with Child C score, MALAT1 expression levels were significantly higher than Child A and B patients ($P < 0.001$ and 0.015, respectively) (Fig. 2C). This was consistent with correlation analysis; moderate positive correlation between MALAT1 and Child score was observed (Pearson correlation coefficient = 0.484, $P = 0.001$). However, AFP level was significantly over-expressed in both Child B and C compared to Child A ($P < 0.001$) (Fig. 2D).

3.2.3. Diagnostic and prognostic value of MALAT1 and AFP

ROC analysis revealed the diagnostic performance of AFP that differentiates cancer patients from normal and cirrhotic individuals at the cutoff values of 131 and 205 ug/L, respectively ($P < 0.001$). Whereas, the prognostic value of AFP to identify class C patients was significant at the cutoff expression level of 650 µg/L with sensitivity of 77.8% and specificity of 61%. On the other hands, serum MALAT1 showed an AUC of 0.57 to discriminate between cirrhotic and normal liver, and an AUC of 0.79 and 0.70 to distinguish patients with cancer from normal and cirrhotic individuals at fold change of 1.0 and 1.26, respectively (Fig. 2(E–H)). The expression level of MALAT1 at 2.54 could discriminate between liver patients with Child C from those with Child B with 66.7% sensitivity and 65.9% specificity (Table 2). It is worth noting that AFP showed better performance than MALAT1 to discriminate between different groups. In our case when we combined both led to model disturbance. This could be due to the limited sample size in the current groups. We recommend replication of such combination in a larger cohort to draw more precise effect estimation.

3.2.4. Association analysis with clinical and biochemical features

In HCC group, higher expression profile of serum MALAT1 was significantly observed in males ($P < 0.001$) and patients with massive

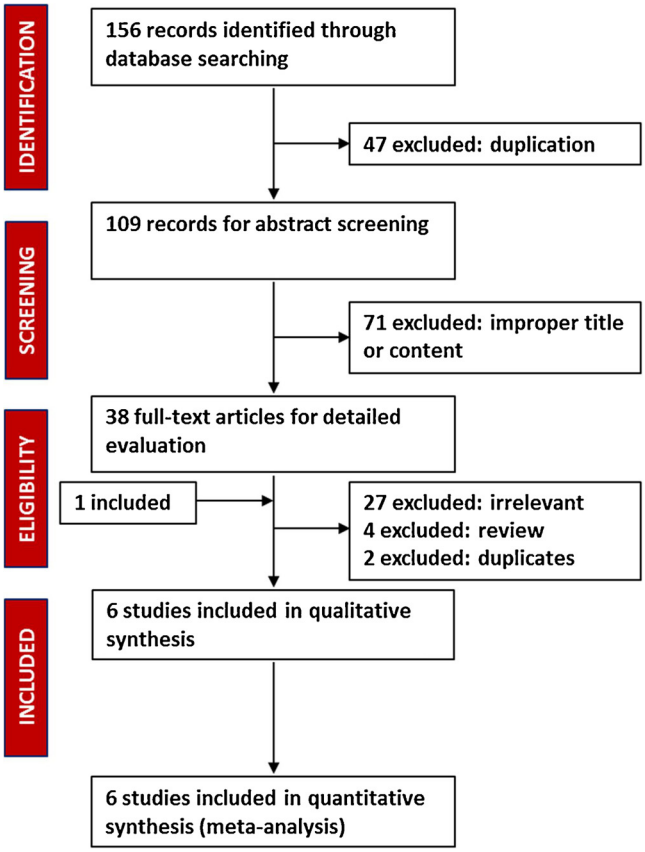


Fig. 5. PRISMA flowchart of the current meta-analysis.

ascites ($P = 0.005$). No association was found with any other demographic, clinical or radiological features (Table 3). Serum MALAT1 levels were positively correlated with liver cell failure score in liver cancer, representing 29.3% of disease variance (r = 0.542, $P = 0.002$, $R^2 = 0.293$) (Fig. 3). A similar trend was observed by principal component analysis for the hepatic cancer patients (Fig. 3C). Correlation analysis of MALAT1 with other biochemical investigations showed positive correlation with total bilirubin (r = 0.456, $P < 0.001$) and AST (r = 0.280, $P = 0.019$), and negative correlation with hemoglobin level (r = 0.312, $P = 0.009$) (Fig. 4).

3.3. The meta-analysis

3.3.1. Study selection and characteristics of eligible studies

The current literature search yielded 156 records. Following the title and abstract screen, 118 duplicates and irrelevant studies were excluded. Thirty-eight articles were retrieved for further evaluation and full text screening. Finally, five case-control studies met our eligibility criteria and were included in this meta-analysis (Fig. 5). The results of the current analysis conducted on an Egyptian population were added. A summary of the six included studies with 12 datasets is demonstrated in Table 4 and Table S1. Studies were conducted in China and Japan during the period between 2012 and 2017. Our study was the only one conducted upon the Arab population. The whole studies were in English language. Sample size ranged from 30 to 112 patients. Three quarters (75.6%) were male patients. For the type of specimens analyzed for MALAT1: 2 studies conducted on blood, 3 on fresh/frozen tissues, and 3 on FFPE tissues. MALAT1 level was detected by qRT-PCR. *In vitro* functional analysis was also performed on nine hepatic cancer cell lines in 4 Chinese studies (Table S1). Knockdown experiments were performed on Huh-6, HepG2, SMMC-7721, Bel-7402, Hep3B, HUH-7, MHCC97L, MHCC97H, and HCCLM3 *via* siRNA transfection. Methodological quality assessment scored from 27 to 29 (out of 32). The Cohen's Kappa coefficient for inter-reviewer agreement of study selection was 0.391 ± 0.279 (95% CI: -0.157 to 0.939), data extraction was 0.576 ± 0.085 (95% CI: 0.410 to 0.742), and for assessment of quality it was 0.333 ± 0.203 (95% CI: -0.064 to 0.731). However, all disagreements were resolved after consensus.

3.3.2. Quantitative data synthesis

A total number of 433 HCC patients (315 tissues and 118 serum/plasma) were analyzed in the meta-analysis for MALAT1 profiling. Expression profile was up-regulated in the whole included studies, in particular blood samples. Three studies reported ROC results with AUC ranged from 0.66 to 0.79. The cut-off values of the high and low expression of MALAT1 in these studies were found to be between 1.0 and 1.6. Pooled effect estimate of MALAT1 was (OR = 3.62, 95% CI: 2.758–4.492, $P < 0.001$) by random-effects model. Heterogeneity was detected between studies (Q = 143.4, df = 6, $P < 0.001$, $I^2 = 95.8\%$) with much variance across the studies (Tau squared = 87%, variance = 0.85) (Fig. 6). Hence, subgroup analysis by sample type was performed. Studies conducted on blood, their effect estimate was 11.4 with 95% CI: 5.6 to 17.3 (fixed model, $P < 0.001$) showing no observed heterogeneity ($I^2 = 0\%$, $P = 0.515$, df = 1). In FFPE studies, the effect estimate was 3.30 (95% CI: 190-4.71) (random model, $P < 0.001$) with major heterogeneity ($I^2 = 94.8\%$, $P < 0.001$, df = 2), whereas

Table 4
Characteristics of included studies in the meta-analysis.

Author	Year	Country	Study design	Sample type	Sample size	HCV/ HBV	F/M	Age < 50/ ≥50 (range)	Fold change (mean ± SD)	AUC	Cutoff value	SE/SP	Quality score	Refs
Toraih	2017	Egypt	P-C	Serum	30	30/0	11/19	9/21 (29-72)	13.12 ± 21.3	0.79	1.00	66.7/80	84.4	[**]
Chen	2017	China	P-C	Fresh/ frozen	56	NA	13/43	11/45	4.9 ± 1.74				87.5	[30]
Li	2016	China	P-C	FFPE	95	NA	20/75	49/46 (29-82)	2.41 ± 0.88	0.65	1.59	89.4/NA	90.6	[31]
Konishi	2016	Japan	P-C	Plasma	88	46/21	37/51	NA (43-86)	9.17 ± 43.6	0.66	1.60	51.1/89.3	87.5	[32]
			P-C	FFPE	20	7/7	NA	NA	3.46 ± 3.08					
Huang	2015	China	P-C	FFPE	32	0/29	2/30	18/14	4.14 ± 1.5				90.6	[33]
Lai	2012	China	P-C	Fresh/ frozen	60	NA	5/55	34/26	2.49 ± 0.78				93.8	[34]
			P-C	Fresh/ frozen	52	NA	NA	NA	NA					

P-C, Patient-control; FFPE, formalin-fixed paraffin embedded sections; HCV, hepatitis C virus; HBV, hepatitis B virus; F/M, female/male; SD, standard deviation; AUC, area under the curve; SE/SP, sensitivity/specificity. All studies were in English language. MALAT1 expression was examined using qRT-PCR in clinical and experimental studies.

** Toraih, 2017 is the current lab work conducted in the study.

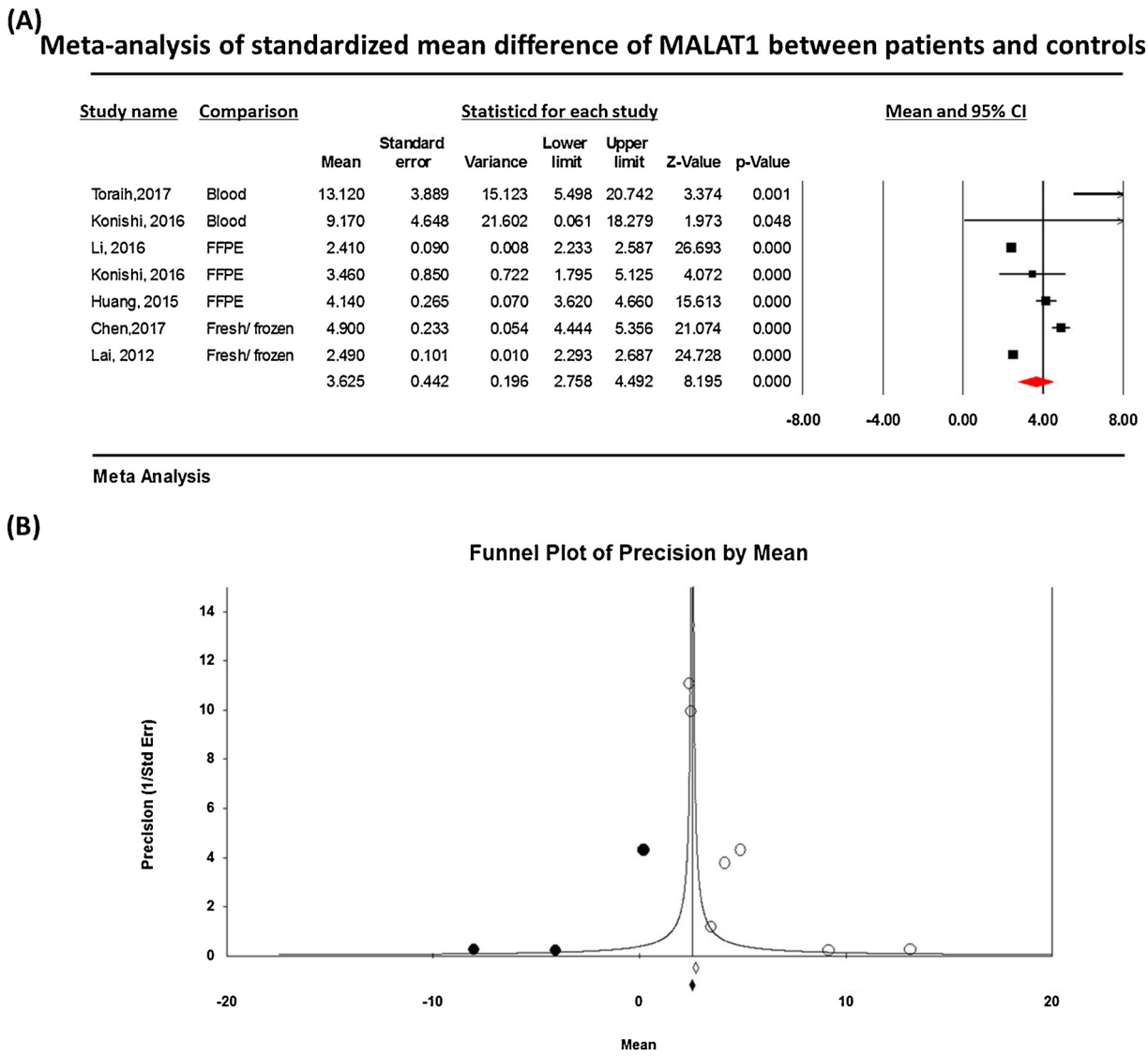


Fig. 6. Quantitative synthesis analysis of the diagnostic value of MALAT1 in HCC. (A) Forest plot of the pooled estimate effect. The random-effects model was used. (OR = 3.62, 95%CI: 2.758–4.492, $P < 0.001$). Heterogeneity was observed across studies (Q = 143.4, df = 6, $P < 0.001$, I2 = 95.8%). (B) Funnel plot for detecting publication bias across studies. Both observed (open circles) and imputed (dark circles) are plotted. Egger's regression test = 0.128, Begg's test = 0.548.

studies using the fresh/frozen samples, point estimate of 2.87 (2.69–3.05) (fixed model, $P < 0.001$) with heterogeneity ($I^2 = 98.8\%$, $P < 0.001$, df = 1).

3.3.3. Association of MALAT1 expression with the clinicopathological features

The pooled effect estimates of the number of tumors (Cohen's d = 0.450, 95% CI (0.21–0.68)), clinical stage (Cohen's d = 0.048, 95% CI (-0.83 to 0.74)), and AFP level (Cohen's d = 0.354, 95% CI (0.1–0.57)) were in favor of the high expression level group. However, no association was observed with any other parameters (Fig. 7). There was no evidence of statistically significant heterogeneity across the studies. Nevertheless, the pooled studies for the clinical stage were heterogeneous due to difference in reporting tumor stage (Q-value = 4.851, df = 2, $P = 0.088$; $I^2 = 58.7\%$) (Table 5).

3.3.4. Publication bias

Begg's funnel plot and Egger's regression test revealed no publication bias across various clinico-pathological parameters except for gender (Begg's test: $P = 0.038$, Egger's test: $P = 0.045$), and tumor size (Begg's test: $P = 0.050$, Egger's test: $P = 0.020$), for which Duval and Tweedie's trim and fill method was applied, with adjusted values similar to the observed ones (Table 6).

4. Discussion

HCC is known with its remarkable ability to metastasize and spread with a high recurrence and poor survival rate [35]. We believe that better understanding of the molecular pathogenesis of HCC may help in the development of more effective treatments to improve the overall prognosis and increase patient survival. Recent studies reported differential expression pattern of lncRNAs between tumor tissues and non-cancer adjacent tissues, suggesting their putative role in the pathogenesis and advancement of cancer [30,31,33,36].

In the experimental part of the current study, we investigated serum expression levels of MALAT1 in HCC patients compared to healthy individuals and cirrhotic patients, and analyze the association between MALAT1 profile and the clinico-pathological features. Our results revealed significant over-expression of MALAT1 in cancer patients. ROC analysis demonstrated better diagnostic and prognostic performance of circulatory MALAT1 in discriminating cancer patients from normal or cirrhotic cohorts, and in differentiating between CTP Class C from Class

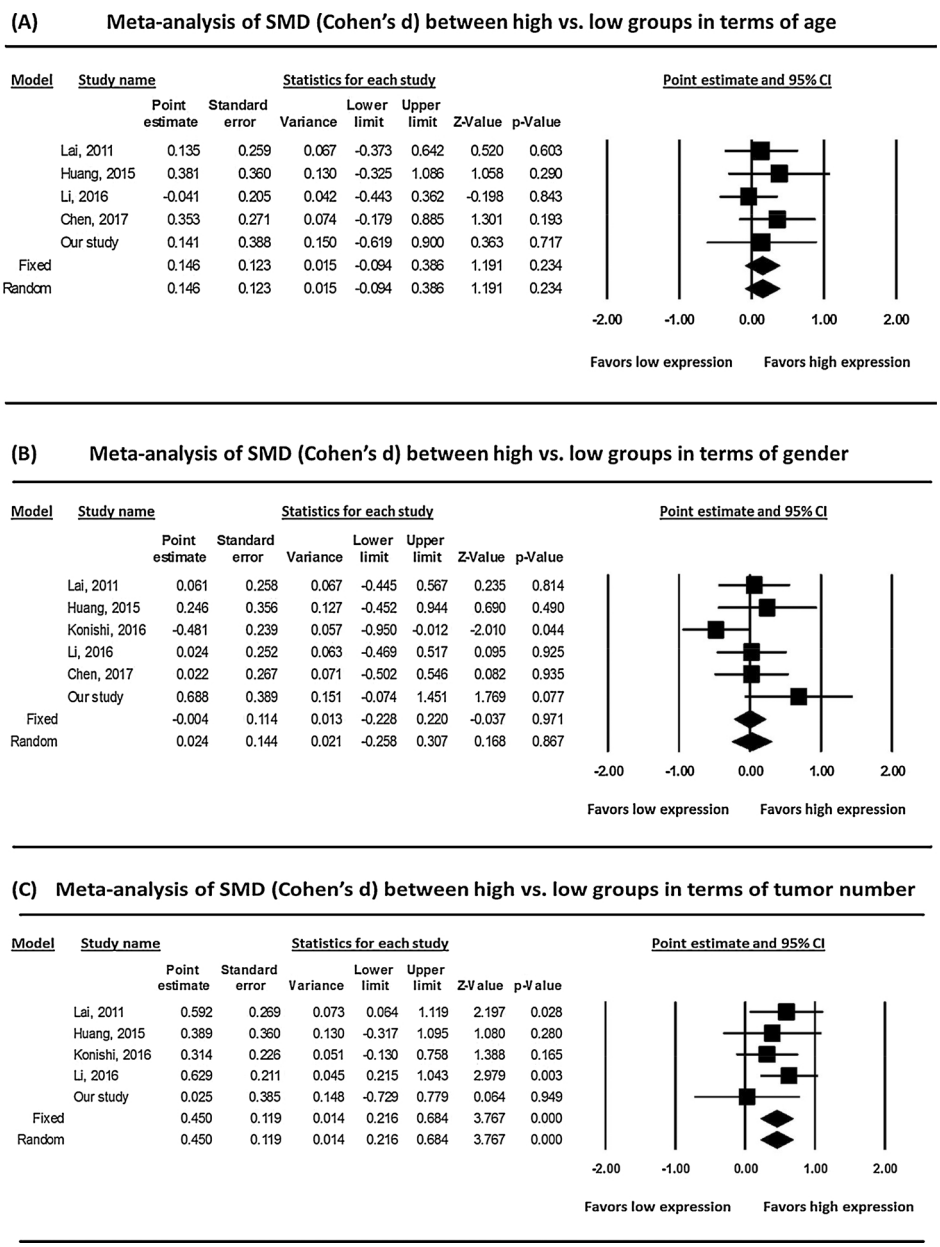


Fig. 7. Pooled estimate of the association of MALAT1 with the clinico-pathological parameters. SMD: standardized mean difference; AFP: alpha fetoprotein, CI: confidence interval.

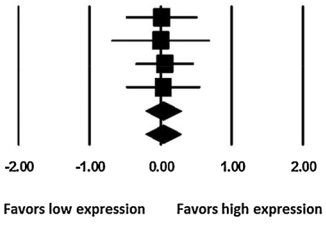
B patients. Notably, combining MALAT1 with AFP biomarker provided more precise diagnostic accuracy. Consistently, MALAT1 up-regulation was documented in HCC, breast, lung, brain, pancreatic, colon, and prostate cancer tissues and cell lines [17,31,33,37,38]. MALAT1 was also found to be highly expressed in peripheral blood mononuclear cells in patients with liver [32], lung [39,40], prostate [41], and pancreatic cancers [42]. During tumor development, cancer cells expel their DNA, mRNAs, and ncRNAs into the circulation by necrosis and apoptosis, resulting in detecting high levels of nucleic acids in the bloodstream and other body fluids of cancer patients which mirror the deregulated patterns in the primary tumor tissues [23,42,43]. Therefore, determining cancer-specific RNA transcripts in the peripheral circulation would provide a useful tool for screening, diagnosis and prognostic stratification.

Another main finding in our study is that serum MALAT1 profile was positively correlated with liver cell failure scores. In addition, higher level was associated with male gender, massive ascites, and AFP level. Nevertheless, no other association with any clinical and biochemical features was found in our population. Similarly, Konishi et al. [32] detected an association of MALAT1 with gender and liver damage classification. Huang et al. [33] and Lai et al. [34] also reported positive correlation between MALAT1 and AFP level. On the other hand, other studies in HCC patients reported association of up-regulated profile with lymph node involvement, advanced clinical stage [31], distant metastasis, and poor overall survival [30]. Interestingly, high level of MALAT1 was an independent predictor of tumor recurrence of HCC after liver transplantation [34] and chemo-resistance in glioblastoma multiforme and colorectal cancer [30,44].

Elevated levels of MALAT1 detected in the study could be caused by chromosomal, genomic, and epigenetic alterations. Chromosomal band 11q13 is considered one of the most commonly amplified genomic regions in human cancer [45]. Increasing gene dosage by amplification is frequently encountered in tumors and is associated with poor prognosis. Amplification in this particular region was reported in 13% of lung cancers, 15% of breast cancer, 21% of bladder carcinoma, 45% of head and neck cancer, and 50% of esophageal cancers [45]. A variant

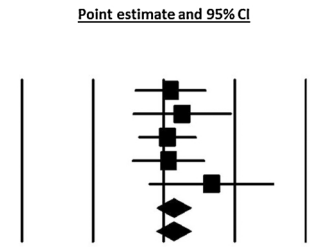
(D) Meta-analysis of SMD (Cohen's d) between high vs. low groups in terms of differentiation

Model	Study name	Point estimate	Standard error	Variance	Lower limit	Upper limit	Z-Value	p-Value
	Lai, 2011	0.015	0.258	0.067	-0.492	0.521	0.057	0.955
	Huang, 2015	0.000	0.354	0.125	-0.693	0.693	0.000	1.000
	Li, 2016	0.058	0.209	0.044	-0.351	0.468	0.279	0.780
	Chen, 2017	0.037	0.267	0.072	-0.487	0.561	0.138	0.890
Fixed		0.035	0.129	0.017	-0.219	0.288	0.268	0.789
Random		0.035	0.129	0.017	-0.219	0.288	0.268	0.789



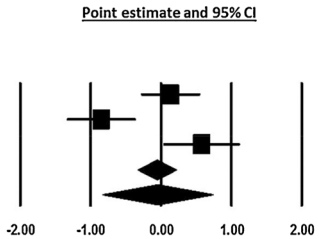
(E) Meta-analysis of SMD (Cohen's d) between high vs. low groups in terms of tumor size

Model	Study name	Point estimate	Standard error	Variance	Lower limit	Upper limit	Z-Value	p-Value
	Lai, 2011	0.095	0.258	0.067	-0.412	0.601	0.366	0.714
	Huang, 2015	0.258	0.357	0.127	-0.441	0.956	0.722	0.470
	Li, 2016	0.053	0.209	0.044	-0.357	0.463	0.254	0.800
	Chen, 2017	0.067	0.262	0.069	-0.447	0.580	0.255	0.799
	Our study	0.673	0.452	0.204	-0.213	1.558	1.489	0.137
Fixed		0.137	0.124	0.015	-0.106	0.380	1.105	0.269
Random		0.137	0.124	0.015	-0.106	0.380	1.105	0.269



(F) Meta-analysis of SMD (Cohen's d) between high vs. low groups in terms of tumor stage

Model	Study name	Point estimate	Standard error	Variance	Lower limit	Upper limit	Z-Value	p-Value
	Konishi, 2016	0.138	0.214	0.046	-0.281	0.556	0.643	0.520
	Li, 2016	-0.849	0.251	0.063	-1.340	-0.357	-3.384	0.001
	Chen, 2017	0.577	0.278	0.077	0.032	1.122	2.075	0.038
Fixed		-0.060	0.140	0.020	-0.335	0.216	-0.425	0.671
Random		-0.048	0.402	0.162	-0.837	0.740	-0.120	0.904



(G) Meta-analysis of SMD (Cohen's d) between high vs. low groups in terms of AFP levels

Model	Study name	Point estimate	Standard error	Variance	Lower limit	Upper limit	Z-Value	p-Value
	Lai, 2011	0.584	0.269	0.072	0.057	1.111	2.171	0.030
	Huang, 2015	0.878	0.386	0.149	0.121	1.635	2.273	0.023
	Konishi, 2016	0.512	0.220	0.048	0.081	0.943	2.327	0.020
	Li, 2016	-0.062	0.225	0.051	-0.503	0.380	-0.274	0.784
	Our study	-0.060	0.385	0.148	-0.815	0.695	-0.156	0.876
Fixed		0.339	0.122	0.015	0.100	0.577	2.786	0.005
Random		0.354	0.175	0.031	0.012	0.697	2.026	0.043

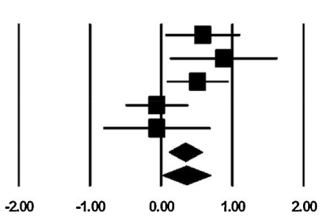


Fig. 7. (*continued*)

(rs619586) in *MALAT1* gene was found to confer protection against HCC in non-drinkers [46]. Another putative mechanism for MALAT1 up-regulation could be gene activation through the binding of various transcription factors (TF) to its promotor. *In vitro* experiments demonstrated the transcriptional activation of MALAT1 *via* the TF specificity protein Sp1/3 in HCC cells. Hence, drugs inhibiting SP proteins, decreased MALAT1 transcription in HepG2 cells and reduced cell viability [33]. In neuroblastoma cell lines, oxytocin mediated the

Table 5
Pooled effect of the association of MALAT1 expression with the clinico-pathological characteristics.

	Association	95% CI		Heterogeneity			
	Cohen's d	Lower limit	Upper limit	Q value	df	*P* values	I^2 (%)
Age of patients	0.145	−0.09	0.38	1.837	4	0.766	0
Gender	0.004	−0.227	0.219	7.716	5	0.173	35.19
Tumor number	**0.450**	0.21	0.68	2.444	4	0.655	0
Tumor grade	0.035	−0.21	0.28	0.029	3	0.999	0
Tumor size	0.137	0.10	0.37	1.78	4	0.776	0
Clinical stage#	**0.048**	−0.83	0.74	4.851	2	0.088	58.7
AFP level	**0.354**	0.10	0.57	7.633	4	0.106	47.59

AFP, alpha fetoprotein, CI, confidence interval, df, degree of freedom. (#) Random-effects model was used due to the presence of inter-study heterogeneity. Bold values indicate statistical significance at $P < 0.05$.

Table 6
The results of Begg's and Egger's tests for the publication bias.

	Begg's test		Duval and Tweedie's trim and fill			Egger's test	
	Z	*P*	Trimmed studies	Observed values (CI)	Adjusted values (CI)	Intercept	*P*
Expression in HCC	0.600	0.548	3	3.62 (2.75-4.49)	2.88 (1.91-3.84)	4.154	0.128
Age of patients	0.979	0.320	3	0.14 (-0.09-0.38)	0.02 (-0.17-0.22)	1.769	0.220
Gender	2.066	**0.038**	2	**−0.004) -0.2-0.21)**	**−0.10 (-0.31-0.09)**	5.459	**0.045**
Tumor number	1.469	0.141	0	0.44 (0.21-0.68)	0.44 (0.21-0.68)	−1.904	0.284
Tumor grade	1.358	0.174	0	0.03 (-0.21-0.28)	0.03 (-0.21-0.28)	−0.412	0.127
Tumor size	1.959	**0.046**	1	**0.13 (-0.1-0.37)**	**0.09 (-0.14-0.32)**	2.241	**0.020**
Clinical stage	0.522	0.601	0	−0.04 (-0.83-0.74)	−0.04 (-0.83-0.74)	1.848	0.944
AFP level	0.979	0.320	0	0.338 (0.1- 0.57)	0.338 (0.1-0.57)	1.046	0.750
5							

AFP, alpha fetoprotein, CI, confidence interval. Bold values indicate statistical significance at $P < 0.0$.

binding of cAMP response element TF to *MALAT1* gene [47]. In bladder carcinoma, TGF-β promoted MALAT1 transcription resulting in its over-expression [48]. Moreover, methylation of the tumor suppressor gene, protocadherin 10 (*PCDH10*), induced the transcription of *MALAT1* gene in endometrial carcinoma *via* the activations of Wnt signaling pathway [49].

Regarding our meta-analysis results, the pooled estimate effect revealed MALAT1 over-expression in liver cancer patients compared to controls. Subgroup analysis by the type of sampling elicited the same results. A significant association of MALAT1 levels was detected with tumor number, clinical stage, and AFP levels. Silencing of MALAT1 in the included hepatic cancer cell lines suppressed cell proliferation, invasion and metastasis, and promoted apoptosis. These findings were in agreement with previous studies which reported that MALAT1 knockdown induced G0-G1 cell cycle arrest, inhibited cell motility [50], decreased the capability of invasion [30], and lead to regulated multidrug resistance through modulating autophagy of HCC cells [51]. MALAT1 silencing also suppressed cell growth, S-phase cell number, and augmented apoptosis in gastric [52] and ovarian cancer [53]. In mammary cancer model, MALAT1 silencing caused a reduction of Her2/neu-amplified tumor organoids, augmented cell adhesion, and loss of cell migration [31].

It has been reported that MALAT1 exhibits its oncogenic function *via* two main mechanisms; (a) alternative splicing modulation [54], and (b) transcriptional regulation of cell cycle and metastatic-related genes [55]. Emerging evidences showed that antisense oligonucleotide (ASO) against MALAT1 in animal models resulted in differential gene expression profiles and altered splicing pattern of genes involved in cellular differentiation and carcinogenic signaling pathways [56]. In HCC, MALAT1 enhanced cellular proliferation and inhibited apoptosis *via* modulating PI3K/AKT and JAK/STAT signaling pathways [50], up-regulating *LTBP3* gene [57], and inhibiting caspase3/7 activity [33]. MALAT1 was found to have a key role in epithelial-mesenchymal transition (EMT) through the regulation of TGF-β and Wnt-catenin signaling pathways [38,48,58,59]. Notably, MALAT1-mediated EZH2 promoted tumor invasion and metastasis in osteosarcoma [60], renal cell carcinoma [61], and colorectal cancer [44]. Moreover, MALAT1 was reported to induce vascular formation and angiogenesis *via* the activation of FGF2 in thyroid cancer [62] and neuroblastoma [63]. The previous mechanisms of action of MALAT1 were depicted in detail in Fig. 8.

Emerging studies reported MALAT1 as a molecular decoy to a wide variety of miRNAs. Inhibiting these miRNAs could result in fine-tuning several cancer-related genes. Our *in silico* analysis identified binding target sites for some miRNAs (miR-1, miR-206, miR-613, and miR-142-3p) that warrant experimental validation. Supporting our bioinformatics prediction, MALAT1 served as a competitive endogenous RNA (ceRNA) to miR-143-3p, which in turn, caused up-regulation of ZEB1 and promoted cancer growth and metastasis in Bel-7402 and HepG2 cell lines [30]. In HCC, binding of MALAT1 to miR-490-3p, maintained the expression level of the cell cycle gene (CDK1) [74]. MALAT1 was tethered with miR-195/EGFR axis and miR-204/SIRT1 axis in human hepatoma cells [50,58]. Furthermore, sponging miR-216b in HCC, switched on *HIF-2a* gene and modulated autophagy [51]. Other MALAT1/target gene interactions are demonstrated in Table S2.

MALAT1 is a key regulatory RNA involved in various biological processes and implicated in many pathological conditions, particularly cancers. Despite the extensive research on this fascinating lncRNA, the precise mechanisms by which it acts to promote tumorigenesis are still obscure. This study is one of a few to provide some insights into the role of MALAT1 in cancers in general, and hepatocellular carcinoma in specific, through a thorough, combined analysis (laboratory, bioinformatic and meta-analysis), allowing for a better understanding of the potential use of this lncRNA in clinical practice. Our study suggests a possible pathogenic role for MALAT1 in HCC. However, due to the limited amount of published literature and small sample size of available reports, further larger studies are recommended to confirm this association as well as to estimate the impact of MALAT1 over-expression on the prognosis of the HCC, its clinical outcomes, patient survival, recurrence, and mortality rates.

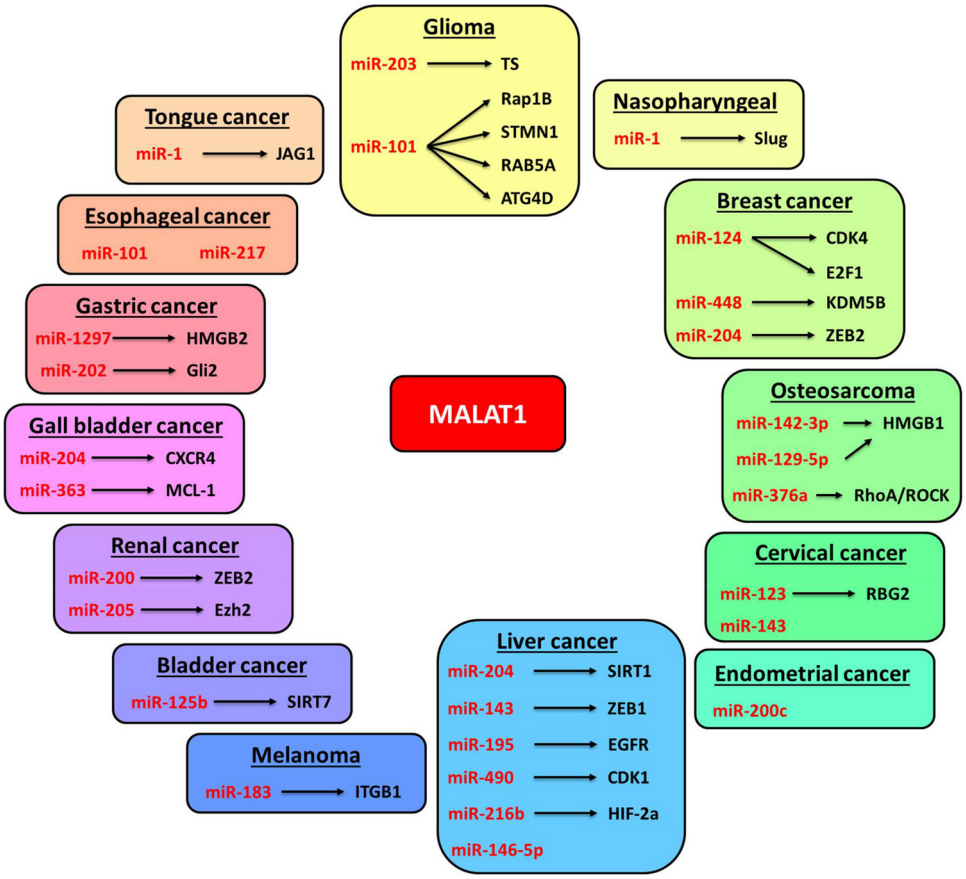


Fig. 8. Molecular Mechanisms of lncRNA MALAT1 action on different cancers. Red colored miRNAs act as competitive endogenous RNAs (ceRNAs) which affect a specific set of target genes (black colored) in each type of human cancers [30,31,38,52,58,61,64–87].

In summary, the current study demonstrated MALAT1 over-expression in HCV-related HCC and its putative oncogenic mechanisms in cancer development and progression. Taking together the results of the meta-analysis, MALAT1 might act as a putative non-invasive biomarker in HCC diagnosis and prognosis, further verification is warranted in future studies.

Conflict of interest

The authors have declared that no competing interests exist.

Funding

The authors received no specific funding for this work.

Acknowledgements

The authors thank the Center of Excellence in Molecular and Cellular Medicine and the Oncology Diagnostic Unit, Suez Canal University, Ismailia, Egypt for providing the facilities for performing the molecular work of the current study.

Appendix A. Supplementary data

Supplementary material related to this article can be found, in the online version, at doi:https://doi.org/10.1016/j.biopha.2018.03.105.

References

[1] S. Shen, Y. Lin, X. Yuan, L. Shen, J. Chen, L. Chen, et al., Biomarker MicroRNAs for diagnosis, prognosis and treatment of hepatocellular carcinoma: A functional survey and comparison, Sci. Rep. 6 (2016) 38311, http://dx.doi.org/10.1038/srep38311.
[2] S. He, D.C. Zhang, C. Wei, MicroRNAs as biomarkers for hepatocellular carcinoma diagnosis and prognosis, Clin. Res. Hepatol. Gastroenterol. 39 (2015) 426–434, http://dx.doi.org/10.1016/j.clinre.2015.01.006.
[3] A. Tang, O. Hallouch, V. Chernyak, A. Kamaya, C.B. Sirlin, Epidemiology of hepatocellular carcinoma: target population for surveillance and diagnosis, Abdom. Radiol. (N.Y.). (2017), http://dx.doi.org/10.1007/s00261-017-1209-1.
[4] K. Jin, T. Li, G. Sánchez-Duffhues, F. Zhou, L. Zhang, Involvement of inflammation and its related microRNAs in hepatocellular carcinoma, Oncotarget 8 (2017) 22145–22165, http://dx.doi.org/10.18632/oncotarget.13530.
[5] H.M. Demerdash, H.M. Hussien, E. Hassouna, E.A. Arida, Detection of MicroRNA in hepatic cirrhosis and hepatocellular carcinoma in hepatitis C genotype-4 in Egyptian patients, Biomed. Res. International. 2017 (2017) 1806069, http://dx.doi.org/10.1155/2017/1806069.
[6] Sun VC-Y, L. Sarna, Symptom management in hepatocellular carcinoma, Clin. J. Oncol. Nurs. 12 (2008) 759–766, http://dx.doi.org/10.1188/08.CJON.759-766.
[7] L. Quagliata, L.M. Terracciano, Liver Diseases and Long Non-Coding RNAs: New Insight and Perspective. Front Med. 1 (2014) 35, http://dx.doi.org/10.3389/fmed.2014.00035.
[8] E.S. Hosseini, M. Meryet-Figuiere, H. Sabzalipoor, H.H. Kashani, H. Nikzad, Z. Asemi, Dysregulated expression of long noncoding RNAs in gynecologic cancers, Mol. Cancer. 16 (107) (2017), http://dx.doi.org/10.1186/s12943-017-0671-2.
[9] E. Bozgeyik, E. Bayraktar, A. Chavez-Reyes, C. Rodriguez-Aguayo, OncoLncs: Long non-coding RNAs with oncogenic functions, Mol. Biol. 5 (162) (2016), http://dx.doi.org/10.4172/2168-9547.1000162.
[10] K. Takahashi, I. Yan, H. Haga, T. Patel, Long non-coding RNA in liver diseases, Hepatology 60 (2014) 744–753.
[11] S.U. Schmitz, P. Grote, B.G. Herrmann, Mechanisms of long noncoding RNA function in development and disease, Cell. Mol. Life Sci. 73 (2016) 2491–2509.
[12] Y. Han, J. Ye, D. Wu, P. Wu, Z. Chen, J. Chen, et al., LEIGC long non-coding RNA acts as a tumor suppressor in gastric carcinoma by inhibiting the epithelial-to-mesenchymal transition, BMC Cancer 14 (2014) 932.
[13] A.K.D.M. Rao, T. Rajkumar, S. Mani, Perspectives of long non-coding RNAs in

cancer, Mol. Biol. Rep. 44 (2) (2017) 203–218.
[14] M. Huarte, The emerging role of lncRNAs in cancer, Nat. Med. 21 (2015) 1253–1261.
[15] L.H. Schmidt, T. Spieker, S. Koschmieder, S. Schaffers, J. Humberg, D. Jungen, et al., The long noncoding malat-1 RNA indicates a poor prognosis in non-small cell lung cancer and induces migration and tumor growth, J. Thorac. Oncol. 6 (12) (2011) 1984–1992.
[16] J. Fellenberg, L. Bernd, G. Delling, D. Witte, A. Zahlten-Hinguranage, Prognostic significance of drug-regulated genes in high-grade osteosarcoma, Mod. Pathol. 20 (10) (2007) 1085–1094.
[17] M.S. Fawzy, E.A. Toraih, H.Y. Abdallah, Long noncoding RNA metastasis-associated lung adenocarcinoma transcript 1 (MALAT1): a molecular predictor of poor survival in glioblastoma multiforme in Egyptian patients, Egypt. J. Med. Hum. Genet. 18 (2017) 231–239.
[18] R. Lin, S. Maeda, C. Liu, M. Karin, T.S. Edgington, A large noncoding RNA is a marker for murine hepatocellular carcinomas and a spectrum of human carcinomas, Oncogene 26 (2007) 851–858.
[19] J.A. Brown, C.G. Kinzig, S.J. DeGregorio, J.A. Steitz, Methyltransferase-like protein 16 binds the 3'-terminal triple helix of MALAT1 long noncoding RNA, Proc. Natl. Acad. Sci. U. S. A. 113 (49) (2016) 14013–14018.
[20] X. Zong, S. Nakagawa, S.M. Freier, J. Fei, T. Ha, S.G. Prasanth, et al., Natural antisense RNA promotes 3′ end processing and maturation of MALAT1 lncRNA, Nucleic Acids Res. 44 (6) (2016) 2898–2908.
[21] J.E. Wilusz, S.M. Freier, D.L. Spector, 3' end processing of a long nuclear-retained non-coding RNA yields a tRNA-like cytoplasmic RNA, Cell 135 (5) (2008) 919–932.
[22] J.M. Lovet, J. Fuster, J. Bruix, The Barcelona approach: diagnosis, staging, and treatment of hepatocellular carcinoma, Liver Transpl. 10 (2) (2004) S115–20.
[23] E.A. Toraih, E.A. Mohammed, S. Farrag, N. Ramsis, S. Hosny, Pilot Study of Serum MicroRNA-21 as a Diagnostic and Prognostic Biomarker in Egyptian Breast Cancer Patients, Mol. Diagn. Ther. 19 (2015) 179–190.
[24] S.A. Bustin, V. Benes, J.A. Garson, J. Hellemans, J. Huggett, M. Kubista, et al., The MIQE guidelines: minimum information for publication of quantitative real-time PCR experiments, Clin. Chem. 55 (2009) 611–622.
[25] E.A. Toraih, M.S. Fawzy, E.A. Mohammed, M.H. Hussein, El-labban MM. MicroRNA-196a2 biomarker and targetome network analysis in solid tumors, Mol. Diagn. Ther. 20 (6) (2016) 559–577.
[26] B. McCune, M.J. Mefford, PC-ORD. Multivariate Analysis of Ecological Data. Version 6, MjM Software, Gleneden Beach, Oregon, U.S.A, 2011.
[27] D. Moher, A. Liberati, J. Tetzlaff, D.G. Altman, PRISMA Group, Preferred reporting items for systematic reviews and meta-analyses: The PRISMA statement, Int. J. Surg. 8 (5) (2010) 336–341.
[28] D.F. Stroup, J.A. Berlin, S.C. Morton, I. Olkin, G.D. Williamson, D. Rennie, et al., meta-analysis of observational studies in epidemiology: A proposal for reporting meta-analysis Of observational studies in epidemiology (MOOSE) group, JAMA 283 (2000) 2008–2012.
[29] X. Yang, X. Xie, Y. Xiao, R. Xie, C.J. Hu, B. Tang, et al., The emergence of long non-coding RNAs in the tumorigenesis of hepatocellular carcinoma, Cancer Lett. 360 (2) (2015) 119–124.
[30] L. Chen, H. Yao, K. Wang, X. Liu, Long non-coding RNA MALAT1 regulates ZEB1 expression by sponging miR-143-3p and promotes hepatocellular carcinoma progression, J. Cell. Biochem. (2017), http://dx.doi.org/10.1002/jcb.26158.
[31] J. Li, H. Yang, X. Cai, Y.-B. Huang, S.-Q. Shen, D.-Y. Wen, et al., Clinical value and function of lncRNA MALAT1 in hepatocellular carcinoma : A comprehensive study with original detection, meta-analysis and in vitro verification, Int. J. Clin. Exp. Pathol. 9 (8) (2016) 7982–7994.
[32] H. Konishi, D. Ischikawa, Y. Yamamoto, T. Arita, K. Shoda, H. Hiramoto, et al., Plasma level of metastasis-associated lung adenocarcinoma transcript 1 is associated with liver damage and predicts development of hepatocellular carcinoma, Cancer Sci. 107 (2) (2016) 149–154.
[33] Z. Huang, L. Huang, S. Shen, J. Li, H. Lu, W. Mo, et al., Sp1 cooperates with Sp3 to upregulate MALAT1 expression in human hepatocellular carcinoma, Oncol. Rep. 34 (5) (2015) 2403–2412.
[34] M.C. Lai, Z. Yang, L. Zhou, Q.Q. Zhu, H.Y. Xie, F. Zhang, et al., Long non-coding RNA MALAT-1 overexpression predicts tumor recurrence of hepatocellular carcinoma after liver transplantation, Med. Oncol. 29 (3) (2012) 1810–1816.
[35] E.A. Toraih, M.S. Fawzy, A.I. El-Falouji, E.O. Hamed, N.A. Nemr, M.H. Hussein, et al., Stemness-related transcriptional factors and homing gene expression profiles in hepatic differentiation and cancer, Mol. Med. 22 (2016) 653–663.
[36] B. Prabhakar, X. Zhong, T.P. Rasmussen, Exploiting long noncoding RNAs as pharmacological targets to modulate epigenetic diseases, Yale J. Biol. Med. 90 (1) (2017) 73–86.
[37] R. Lin, S. Maeda, C. Liu, M. Karin, T.S. Edgington, A large noncoding RNA is a marker for murine hepatocellular carcinomas and a spectrum of human carcinomas, Oncogene. 26 (2007) 851–858.
[38] T.H. Zhang, L.Z. Liang, X.L. Liu, J.N. Wu, K. Su, J.Y. Chen, et al., Long non-coding RNA MALAT1 interacts with miR-124 and modulates tongue cancer growth by targeting JAG1, Oncol. Rep. 37 (4) (2017) 2087–2094.
[39] F. Guo, F. Yu, J. Wang, Y. Li, Y. Li, Z. Li, et al., Expression of MALAT1 in the peripheral whole blood of patients with lung cancer, Biomed. Rep. 3 (3) (2015) 309–312.
[40] D.G. Weber, G. Johnen, S. Casjens, O. Bryk, B. Pesch, K.H. Jockel, et al., Evaluation of long noncoding RNA MALAT1 as a candidate blood-based biomarker for the diagnosis of non-small cell lung cancer, BMC Res. Notes 6 (2013) 518.
[41] S. Ren, F. Wang, J. Shen, Y. Sun, W. Xu, J. Lu, et al., Long non-coding RNA metastasis associated in lung adenocarcinoma transcript 1 derived miniRNA as a novel plasma-based biomarker for diagnosing prostate cancer, Eur. J. Cancer 49 (13) (2013) 2949–2959.
[42] T. Kishikawa, M. Otsuka, M. Ohno, T. Yoshikawa, A. Takata, K. Koike, Circulating RNAs as new biomarkers for detecting pancreatic cancer, World J. Gastroenterol. 21 (2015) 8527–8540.
[43] H. Schwarzenbach, Circulating nucleic acids as biomarkers in breast cancer, BCR 15 (5) (2013) 211.
[44] P. Li, X. Zhang, H. Wang, L. Wang, T. Liu, L. Du, et al., MALAT1 Is Associated with Poor Response to Oxaliplatin-Based Chemotherapy in Colorectal Cancer Patients and Promotes Chemoresistance through EZH2, Mol. Cancer Ther. 16 (4) (2017) 739–751.
[45] X. Huang, S.M. Gollin, S. Raja, T.E. Godfrey, High-resolution mapping of the 11q13 amplicon and identification of a gene, TAOS1, that is amplified and overexpressed in oral cancer cells, Proc. Natl. Acad. Sci. U. S. A. 99 (17) (2002) 11369–11374.
[46] Y. Liu, S. Pan, L. Liu, X. Zhai, J. Liu, J. Wen, et al., A genetic variant in long non-coding RNA HULC contributes to risk of HBV-related hepatocellular carcinoma in a Chinese population, PLoS One 7 (2012) e35145.
[47] T.A. Koshimizu, Y. Fujiwara, N. Sakai, K. Shibata, H. Tsuchiya, Oxytocin stimulates expression of a noncoding RNA tumor marker in a human neuroblastoma cell line, Life Sci. 2010 (86) (2010) 455–460.
[48] Y. Fan, B. Shen, M. Tan, X. Mu, Y. Qin, F. Zhang, et al., TGF-β-induced upregulation of malat1 promotes bladder cancer metastasis by associating with suz12, Clin. Cancer Res. 20 (6) (2014) 1531–1541.
[49] Y. Zhao, Y. Yang, J. Trovik, K. Sun, L. Zhou, P. Jiang, et al., A novel wnt regulatory axis in endometrioid endometrial cancer, Cancer Res. 74 (18) (2014) 5103–5117.
[50] J. Liu, W. Wu, J. Jin, A novel mutation in SIRT1-AS leading to a decreased risk of HCC, Oncol. Rep. 34 (2015) 2343–2350.
[51] P. Yuan, W. Cao, Q. Zang, G. Li, X. Guo, J. Fan, The HIF-2α-MALAT1-miR-216b axis regulates multi-drug resistance of hepatocellular carcinoma cells via modulating autophagy, Biochem. Biophys. Res. Commun. 478 (3) (2016) 1067–1073.
[52] Y. Zhang, Z. Chen, M.J. Li, H.Y. Guo, N.C. Jing, Long non-coding RNA metastasis-associated lung adenocarcinoma transcript 1 regulates the expression of Gli2 by miR-202 to strengthen gastric cancer progression, Biomed. Pharmacother. 85 (2017) 264–271.
[53] L. Wu, X. Wang, Y. Guo, Long non-coding RNA MALAT1 is upregulated and involved in cell proliferation, migration and apoptosis in ovarian cancer, Exp. Ther. Med. 13 (6) (2017) 3055–3060.
[54] L. Hu, Y. Wu, D. Tan, H. Meng, K. Wang, Y. Bai, et al., Up-regulation of long noncoding RNA MALAT1 contributes to proliferation and metastasis in esophageal squamous cell carcinoma, J. Exp. Clin. Cancer Res. 34 (2015) 7.
[55] T. Gutschner, M. Hämmerle, M. Eißmann, J. Hsu, Y. Kim, G. Hung, et al., The noncoding RNA MALAT1 is a critical regulator of the metastasis phenotype of lung cancer cells, Cancer Res. 73 (3) (2013) 1180–1189.
[56] G. Arun, S. Diermeier, M. Akerman, K.C. Chang, J.E. Wilkinson, S. Hearn, et al., Differentiation of mammary tumors and reduction in metastasis upon Malat1 lncRNA loss, Genes Dev. 30 (2016) 34–51.
[57] Z. Hou, X. Xu, L. Zhou, X. Fu, S. Tao, J. Zhou, et al., The long non-coding RNA MALAT1 promotes the migration and invasion of hepatocellular carcinoma by sponging miR-204 and releasing SIRT1, Tumour Biol. 39 (7) (2017) 1010428317718135.
[58] R. Sun, C. Qin, B. Jiang, S. Fang, X. Pan, L. Peng, et al., Down-regulation of MALAT1 inhibits cervical cancer cell invasion and metastasis by inhibition of epithelial-mesenchymal transition, Mol. Biosyst. 12 (2016) 952–962.
[59] J. Liang, L. Liang, K. Ouyang, Z. Li, Yi. MALAT1 induces tongue cancer cells' EMT and inhibits apoptosis through wnt/β-catenin signaling pathway, J. Oral Pathol. Med. 46 (2) (2017) 98–105.
[60] Y. Huo, Q. Li, X. Wang, X. Jiao, J. Zheng, Z. Li, et al., MALAT1 predicts poor survival in osteosarcoma patients and promotes cell metastasis through associating with EZH2, Oncotarget 8 (29) (2017) 46993–47006.
[61] H. Hirata, Y. Hinoda, V. Shahryari, G. Deng, K. Nakajima, Z.L. Tabatabai, et al., Long noncoding RNA MALAT1 promotes aggressive renal cell carcinoma through Ezh2 and interacts with miR-205, Cancer Res. 75 (7) (2015) 1322–1331.
[62] J.K. Huang, L. Ma, W.H. Song, B.Y. Lu, Y.B. Huang, H.M. Dong, et al., LncRNA-MALAT1 Promotes Angiogenesis of Thyroid Cancer by Modulating Tumor-Associated Macrophage FGF2 Protein Secretion, J. Cell. Biochem. (2017), http://dx.doi.org/10.1002/jcb.26153 [Epub ahead of print].
[63] A.E. Tee, B. Liu, R. Song, J. Li, E. Pasquier, B.B. Cheung, et al., The long noncoding RNA MALAT1 promotes tumor-driven angiogenesis by up-regulating pro-angiogenic gene expression, Oncotarget 7 (2016) 8663–8675.
[64] Z. Li, C. Xu, B. Ding, M. Gao, X. Wei, N. Ji, Long non-coding RNA MALAT1 promotes proliferation and suppresses apoptosis of glioma cells through derepressing Rap1B by sponging miR-101, J. Neurooncol. 134 (1) (2017) 19–28.
[65] Z. Fu, W. Luo, J. Wang, T. Peng, G. Sun, J. Shi, et al., Malat1 activates autophagy and promotes cell proliferation by sponging miR-101 and upregulating STMN1, RAB5A and ATG4D expression in glioma, Biochem. Biophys. Res. Commun. 492 (3) (2017) 480–486.
[66] W. Chen, X.K. Xu, J.L. Li, K.K. Kong, H. Li, C. Chen, et al., MALAT1 is a prognostic factor in glioblastoma multiforme and induces chemoresistance to temozolomide through suppressing miR-203 and promoting thymidylate synthase expression, Oncotarget 8 (14) (2017) 22783–22799.
[67] C. Jin, B. Yan, Q. Lu, Y. Lin, L. Ma, The role of MALAT1/miR-1/slug axis on radioresistance in nasopharyngeal carcinoma, Tumour Biol. 37 (2016) 4025–4033.
[68] T. Feng, F. Shao, Q. Wu, X. Zhang, D. Xu, K. Qian, et al., miR-124 downregulation leads to breast cancer progression via LncRNA-MALAT1 regulation and CDK4/E2F1 signal activation, Oncotarget 7 (13) (2016) 16205–16216.
[69] Y. Wang, Y. Zhou, Z. Yang, B. Chen, W. Huang, Y. Liu, Y. Zhang, MiR-204/ZEB2 axis functions as key mediator for MALAT1-induced epithelial-mesenchymal transition

in breast cancer, Tumour Biol. 39 (7) (2017) 1010428317690998.
[70] O.A. Bamodu, W.C. Huang, W.H. Lee, A. Wu, L.S. Wang, M. Hsiao, et al., Aberrant KDM5B expression promotes aggressive breast cancer through MALAT1 overexpression and downregulation of hsa-miR-448, BMC Cancer 16 (2016) 160.
[71] X. Wang, M. Li, Z. Wang, S. Han, X. Tang, Y. Ge, et al., Silencing of long noncoding RNA MALAT1 by miR-101 and miR-217 inhibits proliferation, migration, and invasion of esophageal squamous cell carcinoma cells, J. Biol. Chem. 290 (2015) 3925–3935.
[72] J. Li, J. Gao, W. Tian, Y. Li, J. Zhang, Long non-coding RNA MALAT1 drives gastric cancer progression by regulating HMGB2 modulating the miR-1297, Cancer Cell. Int. 17 (2017) 44.
[73] D. Liu, Y. Zhu, J. Pang, X. Weng, X. Feng, Y. Guo, Knockdown of long non-coding RNA MALAT1 inhibits growth and motility of human hepatoma cells via modulation of miR-195, J. Cell. Biochem. (2017), http://dx.doi.org/10.1002/jcb.26297 [Epub ahead of print].
[74] C. Dou, L. Sun, X. Jin, M. Han, B. Zhang, T. Li, Long non-coding RNA colon cancer-associated transcript 1 functions as a competing endogenous RNA to regulate cyclin-dependent kinase 1 expression by sponging miR-490-3p in hepatocellular carcinoma progression, Tumour Biol. 39 (4) (2017) 1010428317697572.
[75] P. Yuan, W. Cao, Q. Zang, G. Li, X. Guo, J. Fan, The HIF-2α-MALAT1-miR-216b axis regulates multi-drug resistance of hepatocellular carcinoma cells via modulating autophagy, Biochem. Biophys. Res. Commun. 478 (3) (2016) 1067–1073.
[76] X. Tan, Z. Huang, X. Li, Long non-coding RNA MALAT1 interacts with miR-204 to modulate human hilar cholangiocarcinoma proliferation, migration, and invasion by targeting CXCR4, J. Cell. Biochem. 118 (11) (2017) 3643–3653.
[77] S.H. Wang, W.J. Zhang, X.C. Wu, M.Z. Weng, M.D. Zhang, Q. Cai, et al., The lncRNA MALAT1 functions as a competing endogenous RNA to regulate MCL-1 expression by sponging miR-363-3p in gallbladder cancer, J. Cell. Mol. Med. 20 (12) (2016) 2299–2308.
[78] Y. Zhang, X. Tang, M. Shi, C. Wen, B. Shen, MiR-216a decreases MALAT1 expression, induces G2/M arrest and apoptosis in pancreatic cancer cells, Biochem. Biophys. Res. Commun. 483 (2) (2017) 816–822.
[79] L. Zhang, H.E. Niyazi, H.R. Zhao, X.P. Cao, M.N. Abudula, W.J. Ye, et al., Effects of miRNA-143 and the non-coding RNA MALAT1 on the pathogenesis and metastasis of HeLa cells, Genet. Mol. Res. 16 (1) (2017).
[80] S. Liu, L. Song, S. Zeng, L. Zhang, MALAT1-miR-124-RBG2 axis is involved in growth and invasion of HR-HPV-positive cervical cancer cells, Tumour Biol. 37 (2016) 633–640.
[81] Q. Li, C. Zhang, R. Chen, H. Xiong, F. Qiu, S. Liu, et al., Disrupting MALAT1/miR-200c sponge decreases invasion and migration in endometrioid endometrial carcinoma, Cancer Lett. 383 (1) (2016) 28–40.
[82] H. Xiao, K. Tang, P. Liu, K. Chen, J. Hu, J. Zeng, et al., LncRNA MALAT1 functions as a competing endogenous RNA to regulate ZEB2 expression by sponging miR-200s in clear cell kidney carcinoma, Oncotarget 6 (2015) 38005–38015.
[83] Y. Han, Y. Liu, H. Zhang, T. Wang, R. Diao, Z. Jiang, et al., Hsa-miR-125b suppresses bladder cancer development by down-regulating oncogene SIRT7 and oncogenic long noncoding RNA MALAT1, FEBS Lett. 587 (23) (2013) 3875–3882.
[84] K. Liu, J. Huang, J. Ni, D. Song, M. Ding, J. Wang, et al., MALAT1 promotes osteosarcoma development by regulation of HMGB1 via miR-142-3p and miR-129-5p, Cell Cycle. 16 (6) (2017) 578–587.
[85] R. Chen, G. Wang, Y. Zheng, Y. Hua, Z. Cai, Long non-coding RNAs in osteosarcoma, Oncotarget 8 (12) (2017) 20462–20475.
[86] Y. Sun, H. Cheng, G. Wang, G. Yu, D. Zhang, Y. Wang, et al., Deregulation of miR-183 promotes melanoma development via lncRNA MALAT1 regulation and ITGB1 signal activation, Oncotarget 8 (2) (2017) 3509–3518.
[87] S. Bi, C. Wang, Y. Li, W. Zhang, J. Zhang, Z. Lv, et al., LncRNA-MALAT1-mediated Axl promotes cell invasion and migration in human neuroblastoma, Tumour Biol. 39 (5) (2017) 1010428317699796.

Further reading

R. Zhang, H. Hardin, W. Huang, J. Chen, S. Asioli, A. Righi, et al., MALAT1 long non-coding RNA expression in thyroid tissues: analysis by in situ hybridization and real-time PCR, Endocr. Pathol. 28 (1) (2017) 7-12.
Y. Li, Z. Wu, J. Yuan, L. Sun, L. Lin, N. Huang, et al., Long non-coding RNA MALAT1 promotes gastric cancer tumorigenicity and metastasis by regulating vasculogenic mimicry and angiogenesis. Cancer Lett. 395 (2017) 31-44.
Q. Ji, X. Liu, X. Fu, L. Zhang, H. Sui, L. Zhou, et al., Resveratrol inhibits invasion and metastasis of colorectal cancer cells via MALAT1 mediated Wnt/beta-catenin signal pathway, PLoS One. 8 (2013) e78700.
Y. Dong, G. Liang, B. Yuan, C. Yang, R. Gao, X. Zhou, MALAT1 promotes the proliferation and metastasis of osteosarcoma cells by activating the PI3K/Akt pathway, Tumour Biol. 36 (2015) 1477-1486.
S.H. Kim, S.H. Kim, W.I. Yang, S.J. Kim, S.O. Yoon, Association of the long non-coding RNA MALAT1 with the polycomb repressive complex pathway in T and NK cell lymphoma, Oncotarget 8 (19) (2017) 31305-31317.